Chemistry and Biology of Salicylihalamide A and Related Compounds

Larry Yet

Medicinal Chemistry Department, Albany Molecular Research, Inc., P.O. Box 15098, Albany, New York 12212-5098

Received April 28, 2003

Contents

1. Introduction

The use of plant and marine extracts in the search for biologically active natural products continues to be a powerful method for the identification of lead compounds for many chemistry programs in drug discovery.[1,2] Natural products have served as good starting points in developing druglike candidates. One of the initial steps in the development of therapeutic agents is the identification of lead compounds that bind to a receptor or enzyme target of interest. Many analogues of these lead compounds are then prepared and studied in structure−activity relationships (SARs) to define the key recognition elements for maximal activity. Combinatorial chemistry has greatly impacted this drug discovery process during the past decade.[3] Despite this success, compounds originating from natural sources still play a major role in drug therapy. In fact, almost half the drugs on the market are descendants of natural products.[4]

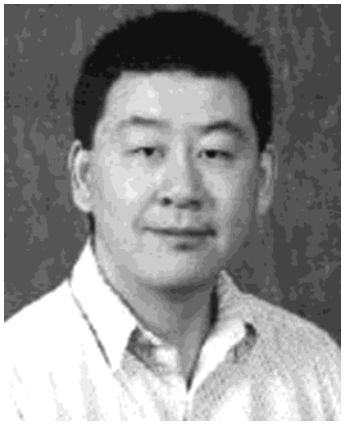

Larry Yet was born in Vancouver, British Columbia, Canada. After graduating with his B.Sc. degree in chemistry from the University of British Columbia, working with Professor James P. Kutney on his senior thesis, he continued his graduate studies with Professor Harold Shechter at The Ohio State University, receiving his M.S. degree in 1990 and Ph.D. in 1995. He then carried out postdoctoral research with Professor Douglass F. Taber at the University of Delaware. Since 1996, he has worked at Albany Molecular Research, Inc. as a Senior Research Scientist.

In 1997, Boyd and co-workers at the Laboratory of Drug Discovery Research and Development at the National Cancer Institute reported the bioassay-guided isolation of salicylihalamide A (**1a**) from an unidentified species of the marine sponge *Halicona* (Figure 1).[5] Salicylihalamide A (**1a**) was accompanied by a small amount of salicylihalamide B (**1b**) with a (*Z*)-enamide double bond. The structure was determined by NMR spectroscopic methods, and the absolute stereochemistry was assigned by the use of Mosher esters. The structures were originally assigned as the enantiomeric structures shown as **1a** and **1b** as a result of the failure to take into account the priority order change on conversion of the acid chloride to the ester.[6] As a result, the biologically active forms are thus assigned as (−)-salicylihalamide A (**2a**) and (−)-salicylihalamide B (**2b**). (−)-Salicylihalamide A (**2a**) showed an unique differential cytotoxicity profile in the NCI 60-cell line human tumor assay.[5] The mean GI_{50} concentration was 15 nM, with a range of differential sensitivity $\leq 10^3$. The melanoma cell lines showed the highest average sensitivity ($GI_{50} = 7$ nM, TGI = 60 mM). The mean-graph profiles of **2a** showed no significant correlations to those of any other antitumor compounds contained in the NCI database, suggesting a new mechanism of action.

These were the first examples of a growing number of structurally related macrocyclic salicylate natural

10.1021/cr030035s CCC: $44.00
Published on Web 09/26/2003

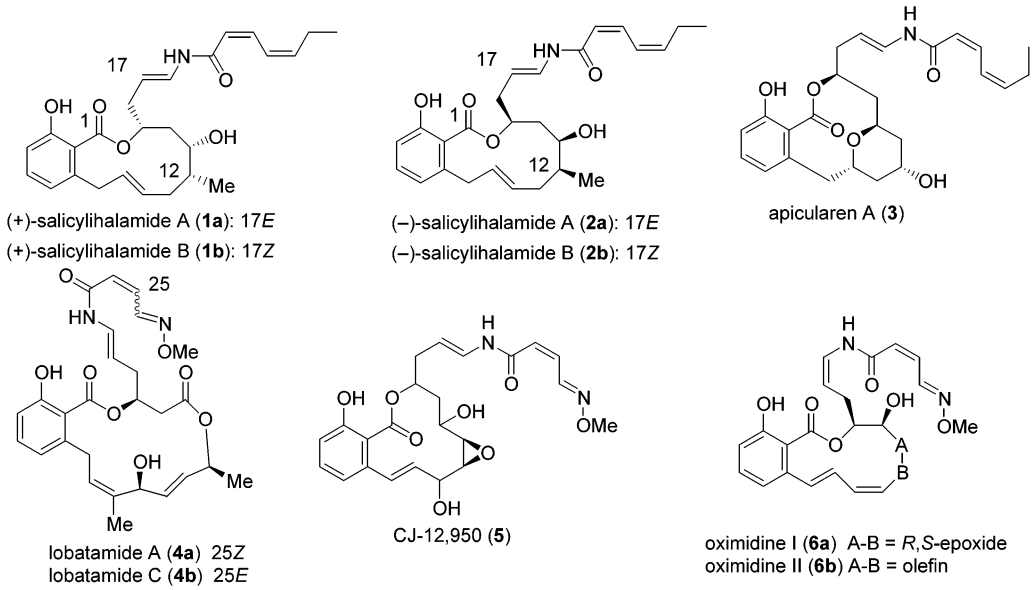

Figure 1. Salicylihalamide A (**2a**) and structurally related natural products.

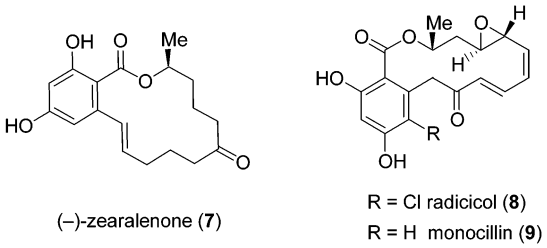

Figure 2. Structures of similar macrocyclic salicylic acid lactones.

products. Apicularen A (**3**) was isolated from a myxobacteria and was chosen for study on the basis of its extremely potent cytostatic activity against human cancer cell lines, including a multi-drug-resistant cervix carcinoma cell line.[7] Phenotypes associated with apicularen A (**3**) treatment include potent growth inhibition of human cell lines ($IC_{50} \approx 0.1-3$ ng/mL), the induction of an apoptotic-like cell death sequence, and the formation of mitotic spindles with multiple spindle poles and clusters of bundled actin from the cytoskeleton. Lobatamide A (**4a**) and lobatamide C (**4b**) and its congeners in three different tunicate species of the genus *Aplidium* exhibit a mean GI_{50} concentration of 1.6−15 nM, with a range of differential sensitivity $\geq 10^3$.[8] Pfizer Pharmaceuticals isolated the fungal metabolites CJ-12,950 (**5**) and CJ-13,357 on the basis of their ability to induce low-density lipoprotein (LDL) receptor gene expression, an observation that has potential relevance to the treatment of hypercholesterolemia and hyperlipidemia.[9] Oximidines I (**6a**) and II (**6b**) have been shown to induce selective growth inhibition of oncogene-transformed rat fibroblasts (3Y1 cells) at 15- to 30-fold lower concentrations than for the parent cell line.[10]

Other macrocyclic salicylic acid lactones that are structurally similar to the salicylihalamides A and B, including (−)-zearalenone (**7**),[11,12] radicicol (**8**)[13,14] and monocillin (**9**),[13,14] are shown in Figure 2. (−)-Zearalenone (**7**) has been found to possess anabolic, estrogenic, and antibacterial activities.[11] Both radicicol (**8**) and monocillin (**9**) exhibit a variety of antifungal and antibiotic properties.[13] Recently, the antitumor properties of radicicol (**8**) have come into focus. This compound has the ability to suppress the transformed phenotype caused by various oncogenes such as *src*, *ras*, and *raf*, which have been linked to its high-affinity binding (20 nM) and inhibition of the Hsp90 molecular chaperone.[15] This "anti-chaperone" activity may stimulate depletion of oncogenic proteins and could therefore be of clinical interest.

These attractive biological properties of the structurally related macrolactones render these targets desirable for total syntheses and serve as excellent scaffolds for the development and validation of new synthetic methodologies. This review will cover the chemical synthesis of these unique biological classes of natural products. Biological studies relating to these classes of natural products will also be surveyed.

2. The Chemistry of the Salicylihalamides

2.1. The Ring-Closing Metathesis Approach

The salicylihalamides and their biosynthetically related macrocyclic salicylate congeners represent a structurally novel class of macrocyclic benzolactones incorporating salicylic acid with an unusual, highly unsaturated *N*-acyl enamine side chain. To date, the reported total syntheses of the salicylihalamides have required the installation of this highly sensitive chain moiety at a late stage. The total syntheses published thus far all rely on a ring-closing metathesis (RCM) reaction[16] as the pivotal key step, although other key transformations are showcased in the synthesis of the macrolactone templates. The general route for the total syntheses of (−)-salicylihalamides A (**2a**) and B (**2b**) is presented in Scheme 1. Salicylic acid derivatives **10** are coupled with diastereomerically pure alcohols **11** under Mitsunobu conditions to give salicylate esters **12**. Esters **12** then participate in a ring-closing metathesis reaction to provide macro-

Scheme 1. General Scheme for Mitsunobu Coupling/Ring-Closing Metathesis/Enamide Side-Chain Installation Approaches to the Syntheses of Salicylihalamides A (2a) and B (2b)

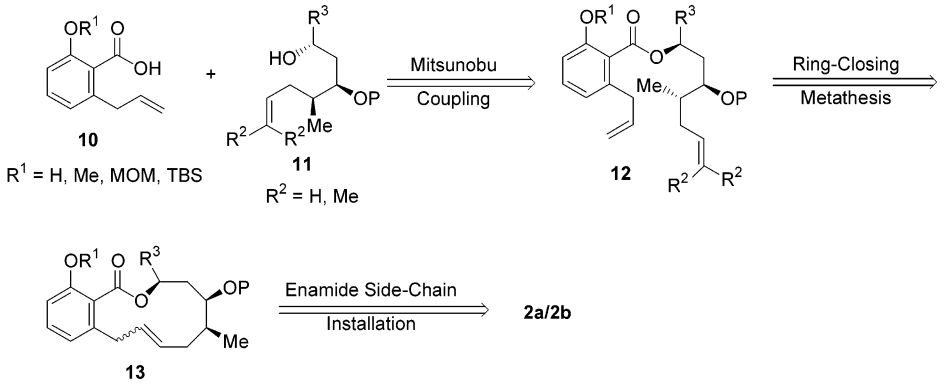

Scheme 2. Various Approaches to the Salicylic Acid Precursors

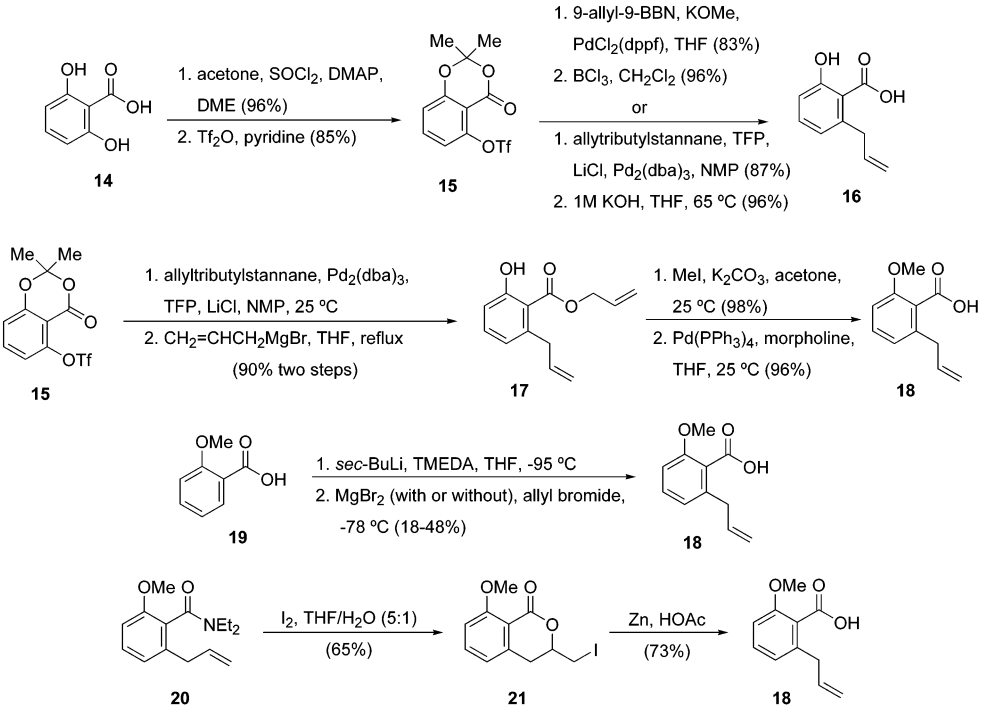

lactones **13**, which are then followed by enamide side-chain installation to complete the total syntheses of **2**.

A detailed discussion of the chemical syntheses of the salicylic acid precursors **10** and the diastereomerically pure alcohol partners **11** will be presented, followed by the total syntheses of **2a/2b** via the ring-closing metathesis reaction. Scheme 2 outlines the various approaches to the preparation of the salicylic acid precursors **10**. Fürstner and co-workers employed inexpensive 2,6-dihydroxybenzoic acid (**14**) as the starting material, which was converted on a multigram scale to triflate **15** by formation of the isopropylidene intermediate followed by reaction with triflic anhydride.[17] Triflate **15** was allylated in high yield by a modified Suzuki-type reaction with potassium methoxide as the base; cleavage of the isopropylidene moiety of **15** with boron trichloride gave the salicylic acid derivative **16**. Alternatively, Snider and Song prepared **16** by Stille coupling of triflate **15** with allyltributylstannane using $Pd_2(dba)_3$ and tri(2-furyl)-phosphine and hydrolysis of the acetonide under basic conditions.[18] De Brabander utilized triflate **15** in a palladium-catalyzed allylation, followed by a Grignard addition to give allyl ester **17**.[19] Methylation of **17**, followed by deprotection of the allyl group, afforded salicylic acid precursor **18**. Several research groups conveniently prepared salicylic acid precursor **18** in variable yields by ortho metalation of **19** using *sec*-butyllithium, followed by trapping of the resulting aryllithium species with allyl bromide at low temperatures with or without the use of magnesium bromide.[17,20,21] Smith and Zheng took the known amide **20**[22] in the presence of iodine in aqueous tetrahydrofuran mixture to furnish iodolactone **21**, which was then converted to salicylic acid derivative **18** on treatment with zinc in acetic acid.[23]

Many different routes have been investigated for the syntheses of diastereomerically pure alcohol partners for the key-forming Mitsunobu reaction. De Brabander and co-workers prepared the requisite alcohol by the route shown in Scheme 3.[19] Enantioselective allylation of aldehyde **22** gave the intermediate homoallyl alcohol, which underwent silyl pro-

Scheme 3. Synthesis of the Diastereomerically Pure Alcohol Precursor 26 (De Brabander and Co-workers)

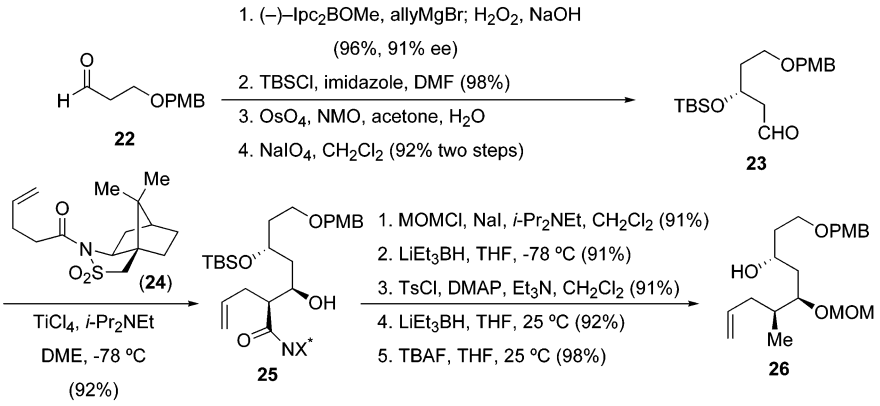

Scheme 4. Synthesis of the Diastereomerically Pure Alcohol Precursor 32 (Fürstner and Co-workers)

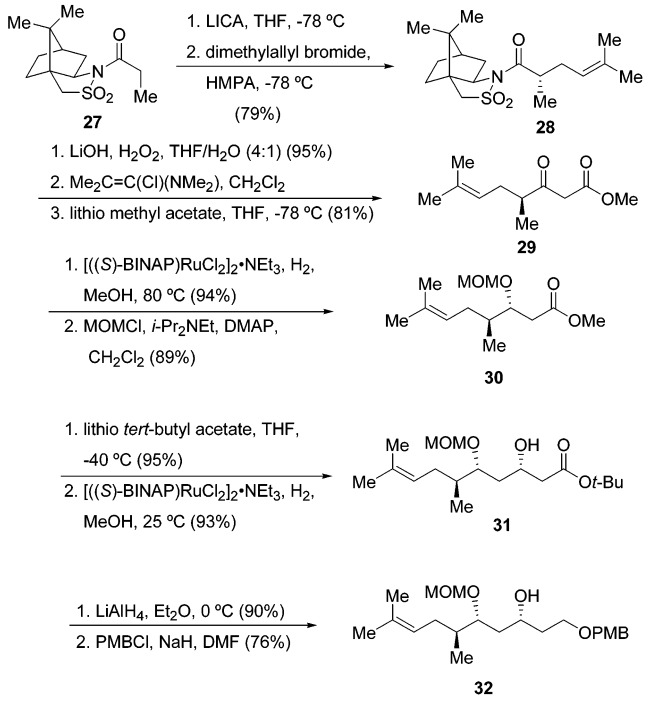

tection and oxidative double-bond cleavage to give aldehyde **23**. Treatment of this aldehyde with the (*Z*)-*O*-titanium enolate derived from (2*S*)-*N*-(4-pentenoyl)bornanesultam **24** produced exclusively one diastereomeric aldol product, **25**, in 92% yield. Alcohol protection of **25**, followed by reductive chiral auxiliary removal, tosylation, reduction, and silyl deprotection, furnished the requisite alcohol **26**.

Fürstner prepared the Mitsunobu coupling precursor **32** by the route outlined in Scheme 4.[17] Prenylation of Oppolzer's bornanesultam **27** delivered diastereoselectively compound **28**. Saponification of **28**, conversion of the resulting acid to the acid chloride, and chain extension with lithio methyl acetate provided β-oxo ester **29**, which underwent a chemo- and stereoselective hydrogenation in the presence of chiral ruthenium BINAP catalyst, followed by MOM-ether formation to give ester **30**. The stage was then set for the iterative construction of the remaining stereocenter. Chain extension of **30** with the lithium enolate of *tert*-butyl acetate, followed by a diastereoselective reduction of the resulting β-keto ester with the same ruthenium BINAP catalyst, furnished the β-hydroxy ester **31**. Reduction with lithium aluminum hydride and protection with *p*-methoxybenzyl chloride gave the desired mono-PMB ether derivative **32**.

Smith and Zheng synthesized the diastereomerically pure alcohol **38** by the route presented in Scheme 5.[23] Aldehyde **33**, readily prepared from (*S*)-malic acid in three steps,[24] underwent Roush crotylboration with allyl boronate **34** to provide alcohol **35** in 90% diastereoselectivity. Alcohol **35** was elaborated to homologated alkene **36** by TBS protection, hydroboration, Swern oxidation, and Wittig methylenation. Acetonide deprotection of **36** with aqueous trifluoroacetic acid gave the intermediate diol, which was converted to the terminal epoxide **37** using the Kishi protocol. Treatment of epoxide **37** with the vinyl Grignard in the presence of a catalytic amount of copper(I) iodide afforded the secondary alcohol **38**.

Labrecque and co-workers prepared the alcohol precursor **42**, as shown in Scheme 6.[20] The known epoxide **39**[25] was transformed in a one-pot procedure to the protected 1,3-diol **40** via sequential reduction and in situ protection with *p*-anisaldehyde. A series of steps involving cleavage of **40** with DIBALH, Dess−Martin oxidation, Roush crotylation, TBS protection, and hydroboration furnished alcohol **41** in good overall yield. Dess−Martin oxidation of alcohol **41**, followed by Wittig homologation and PMB deprotection with DDQ, afforded requisite partner **42**.

Snider and Song prepared the Mitsunobu cyclic ether precursor **49** as outlined in Scheme 7.[18] Reduction of amide **43**, prepared by Myers's procedure from allyl bromide and (−)-pseudoephedrine propanamide, and Swern oxidation provided aldehyde **44**.[26] Asymmetric Carreira aldol condensation of **45** with aldehyde **44** furnished an inseparable 4.2:1 mixture of *syn*:*anti* alcohols **46**, which was converted to β-keto ester **47** under solvent reflux. β-Keto ester **47** was then reduced to the syn alcohol and cyclized to the hydroxy lactone **48**. Reduction to the lactol and methyl protection afforded cyclic ether **49**.

Georg and co-workers synthesized the lactone precursor **52** by the route shown in Scheme 8.[21] The known alcohol **50**, prepared in five straightforward steps from diacetone-D-glucose,[27] was converted to its triflate and reacted with a higher order allylcyanocuprate to provide **51** with inversion of configuration.

Scheme 5. Synthesis of the Diastereomerically Pure Alcohol Precursor 38 (Smith and Zheng)

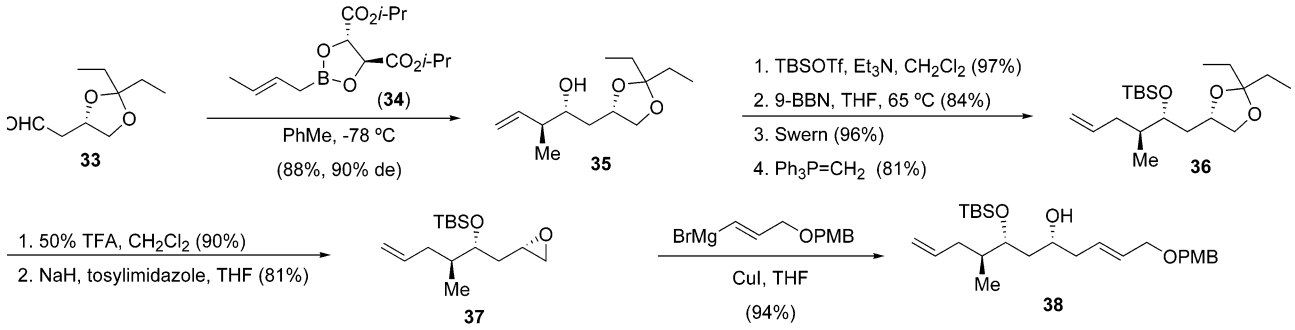

Scheme 6. Synthesis of the Diastereomerically Pure Alcohol Precursor 42 (Labrecque and Co-workers)

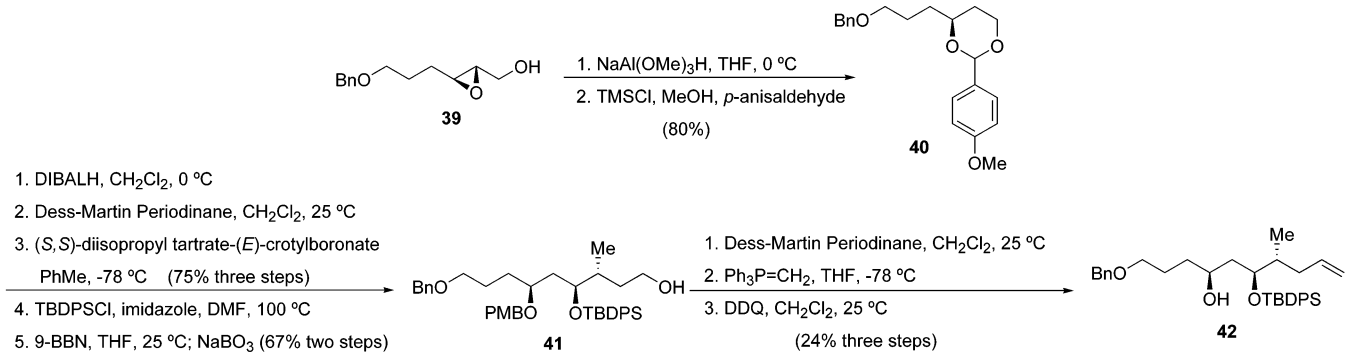

Scheme 7. Synthesis of the Diastereomerically Pure Alcohol Precursor 49 (Snider and Song)

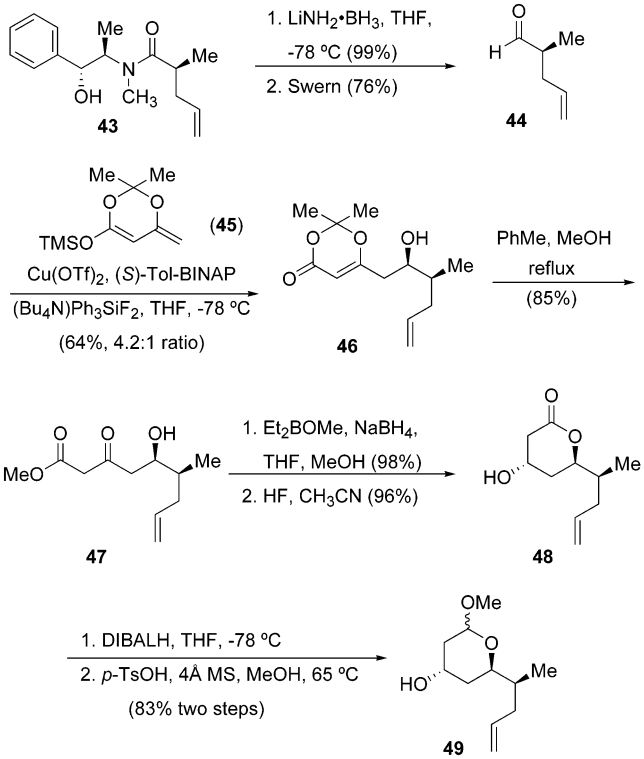

Scheme 8. Synthesis of the Diastereomerically Pure Alcohol Precursor 52 (Georg and Co-workers)

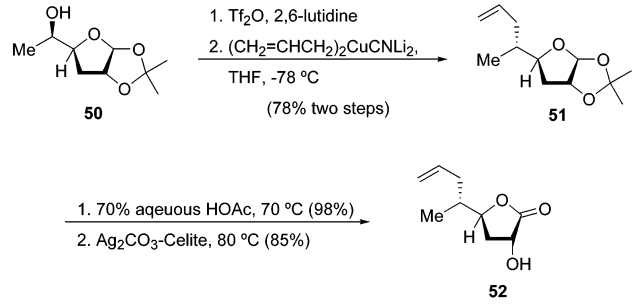

Acetonide deprotection of **51** and subsequent selective oxidation of the anomeric hydroxy group with a silver carbonate−Celite combination afforded lactone **52** in excellent yield.

With these salicylic acid precursors and diastereomerically pure alcohols available, total syntheses of **2** have been completed by several research groups. De Brabander and co-workers condensed protected allylsalicylic acid **18** (R = Me) or **53** (R = MOM) with alcohol **26** to give diene precursor **54a** or **54b** under Mitsunobu conditions (Scheme 9).[19] Ring-closing metathesis of diene **54a** or **54b** with ruthenium catalysts **55** or **56** (see Figure 3) gave (*E*)-macrolactone **58** and (*Z*)-macrolactone **58** in various ratios which could be separated by silica gel chromatography. It was observed that the first-generation ruthenium catalyst **55** gave a higher *E*/*Z* ratio than the second-generation ruthenium catalyst **56**. Elaboration of isomer **58*E*** to TBS-protected isocyanate **59**, followed by addition of lithiated vinyl bromide **60** and TBS deprotection, afforded the first reported total synthesis of (−)-salicylihalamide A (**2a**) and salicylihalamide B (**2b**).

Fürstner and co-workers employed a similar methodology in the total synthesis of (−)-salicylihalamide A (**2a**).[17] 6-Allylsalicylic acid (**16**) was coupled with alcohol **32** under Mitsunobu conditions, followed by phenol protection, to yield a series of diene precursors **61** (Scheme 10). Ring-closing metathesis of **61** with second-generation ruthenium catalyst **57** afforded benzolactone **62** in various *E*/*Z* ratios. Without phenol

Scheme 9. Ring-Closing Metathesis of Diene 54a or 54b in the Total Synthesis of (−)-Salicylihalamide A (De Brabander and Co-workers)

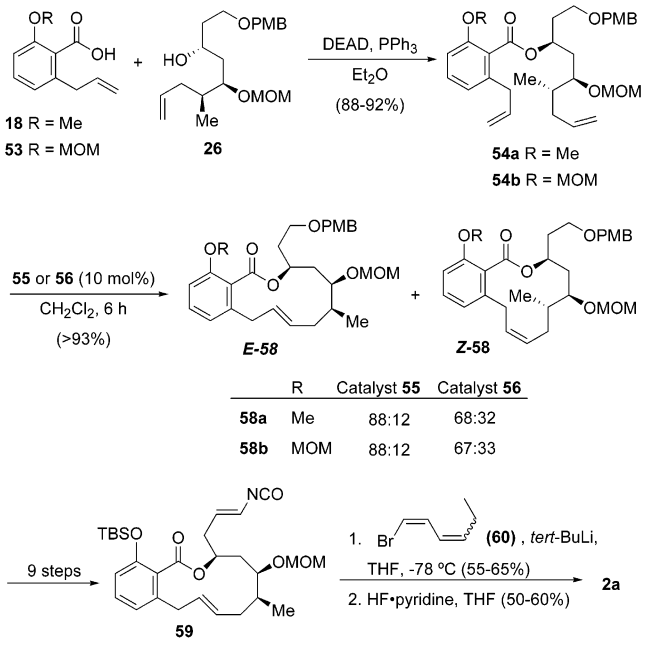

protection, (*Z*)-benzolactone **62a** was observed exclusively. At the time of publication, a conclusive explanation for the observed stereochemical results could not be provided. Elaboration of **62** to vinyl iodide **63**, followed by copper-catalyzed cross coupling with amide **64**, afforded (−)-salicylihalamides A (**2a**) and B (**2b**) in 57% isolated yield (**2a**:**2b** ca. 2.5:1).

Smith and Zheng accomplished the union of acid **18** and alcohol **38** to provide the olefin metathesis substrate **65** under Mitsunobu conditions (Scheme 11).[23a] RCM of diene **65** with Grubbs's catalyst **55** provided the salicylihalamide macrolide **66** in an *E*/*Z* ratio of 10:1 in 85% combined yield. Elaboration of **66** to enamine **67**, followed by acylation with acid chloride **68** and sequential TBS deprotections, afforded (−)-salicylihalamide A (**2a**). The first-generation synthesis of (+)-salicylihalamide A (**1a**) was also accomplished by a similar route using the other diastereomer.[23b]

Labrecque and co-workers prepared the cyclization precursor **69** from Mitsunobu coupling of acid **18** with alcohol **42**, which upon RCM with Grubbs's catalyst **55** afforded benzolactone **70** with an *E*/*Z* ratio of 9:1 (Scheme 12).[20] Benzolactone **70** was transformed to aldehyde **71** in three steps and was condensed with amide **64** to give *N*,*N*′-bis-acylated aminal **72**. This compound underwent elimination and concomitant silyl removals on treatment with sodium hydride in benzotrifluoride to afford (+)-salicylihalamides A (**1a**) and B (**1b**), which were separated by preparative high-pressure liquid chromatography. This same sequence was applied to the enantiomer of **42** to give the natural (−)-salicylihalamides A (**2a**) and B (**2b**).

Snider and Song applied the Mitsunobu coupling protocol to 6-allylsalicylic acid (**16**) with cyclic ether **49** to afford diene **73** (Scheme 13).[18] RCM of **73** did not proceed, presumably because the diequatorial substituents on the tetrahydropyran ring keep the alkenes too far apart for interaction. Acid hydrolysis of **73** to the lactol, followed by alkene homologation and TBS protection, yielded diene precursor **74**. Ring-closing metathesis of **74** with ruthenium catalyst **55** afforded macrolactone **75** in an *E*/*Z* ratio of 4:1, which was separated by flash column chromatography. (−)-Salicylihalamide A (**2a**) was then synthesized in eight steps from macrolactone **75**.

Georg and co-workers showed that the Mitsunobu coupling of 6-allylsalicylic acid (**16**) with lactone **52** provided the cyclization precursor diene **76** (Scheme 14).[21] Unfortunately, all attempts to utilize the ring-closing metathesis reaction on substrate **76** failed to deliver any of the desired benzolactone. However, protection of the phenol and reduction of the lactone furnished lactol **77**, which underwent smooth RCM with Grubbs's ruthenium catalyst **55** to afford benzolactone **78** in 60% yield with a 7:3 *E*/*Z* ratio.

Despite the excellent advances in the ring-closing metathesis reaction,[16] there is a general lack of stereochemical predictive model for the controlled *E*/*Z* geometric formation of large rings formed by this mode of cyclization. It is quite clear that ruthenium catalysts **55**, **56**, and **57** all efficiently performed the cyclizations in excellent yields, albeit with different degrees of *E*/*Z* selectivities. Several observations could be noted in Table 1, where various groups on the salicylic acid, C-13 and C-15 positions, and the olefin moieties plus the choice of ruthenium catalysts influence the outcome of geometrical ratios of resulting olefin products. In general, if the hydroxy group of the salicylic acid portion is substituted and C-15 is functionalized, the use of first-generation ruthenium catalyst **55** (entries 1, 3, 9, and 10) gives higher *E*/*Z* ratios (>80:20) than that of the second-generation ruthenium catalysts **56** or **57** (~40:60 to 70:30). When the olefins are trisubstituted, as in **61a**−**d** (entries 5−8), the more reactive catalyst **57** had to be employed for the reaction to proceed. However, when the salicylic acid portion is not protected, the (*Z*)-isomer is obtained exclusively (entry 5). Fürstner has speculated that the formation of the hydrogen bond between the phenolic OH and the COOR group prevented free rotation in this part of the molecule, forcing a strongly preferred conformation of the cyclization precursors or the ruthenium chelated to the OH, resulting in phenolate complex formation.[17]

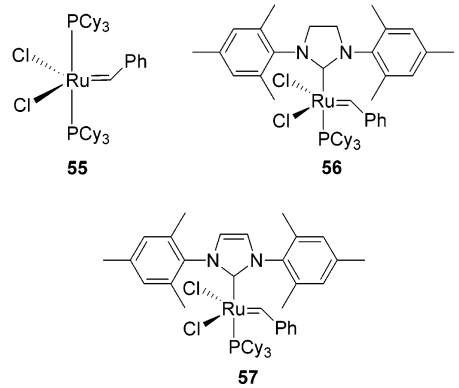

Figure 3. Structures of ring-closing metathesis ruthenium catalysts.

Scheme 10. Ring-Closing Metathesis of Diene 61 in the Total Synthesis of (−)-Salicylihalamide A (Fürstner and Co-workers)

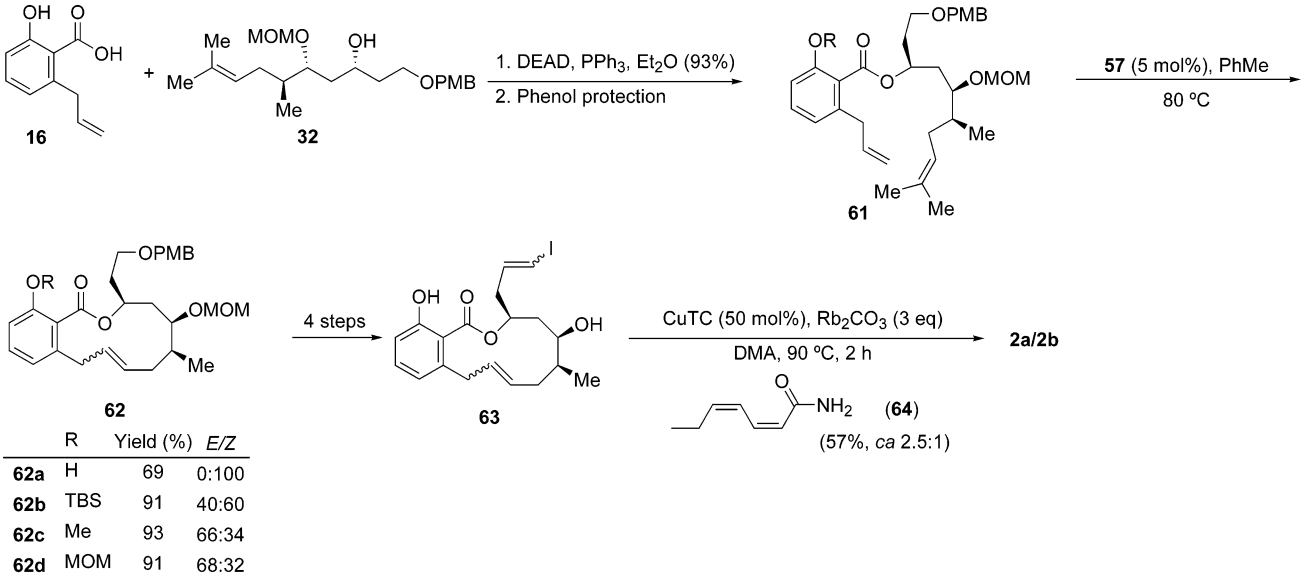

	R	Yield (%)	*E/Z*
62a	H	69	0:100
62b	TBS	91	40:60
62c	Me	93	66:34
62d	MOM	91	68:32

Scheme 11. Ring-Closing Metathesis of Diene 65 in the Total Synthesis of (−)-Salicylihalamide A (Smith and Zheng)

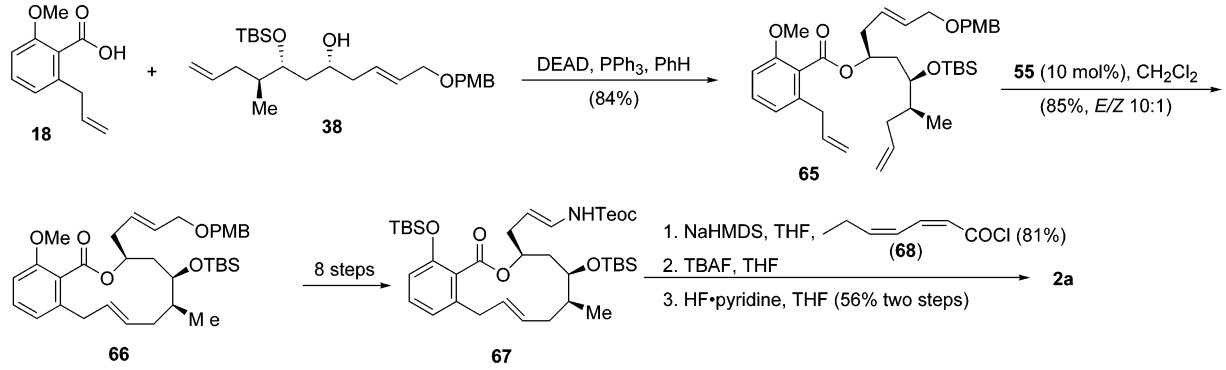

Scheme 12. Ring-Closing Metathesis of Diene 69 in the Total Synthesis of (+)-Salicylihalamide A (Labrecque and Co-workers)

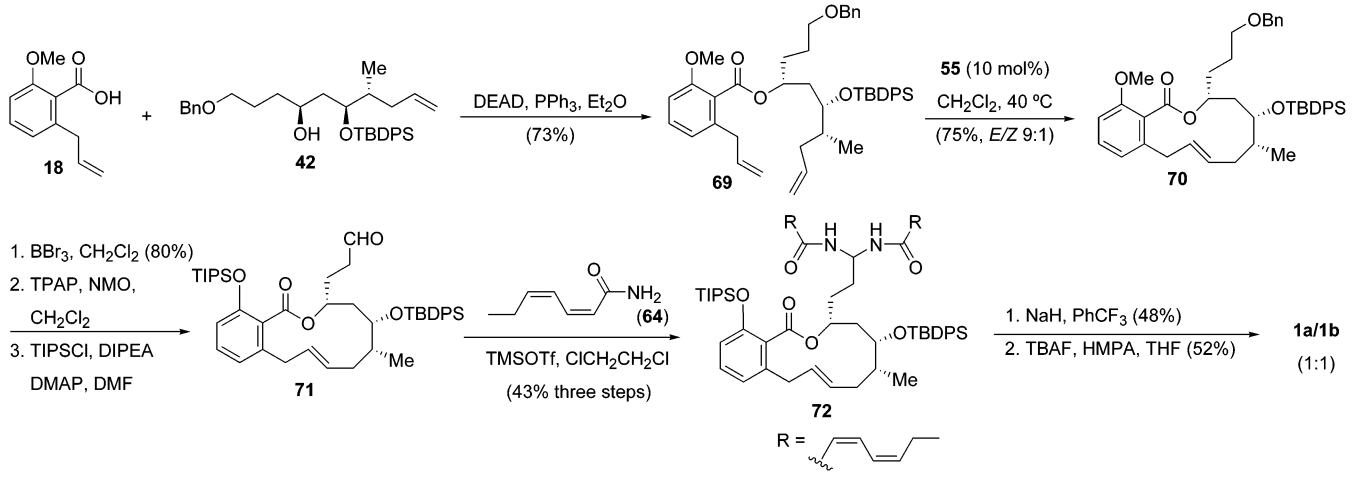

De Brabander has suggested reasons for the different *E*/*Z* selectivities depending on the choice of ruthenium catalysts.[19] RCM-based macrocyclizations are known to be reversible processes, usually providing products of different *E*/*Z* mixtures, often favoring the thermodynamically more stable isomer.[28] Also, in principle, a thermodynamic distribution of products is produced if there are secondary metathetical isomerizations that can compete on the time scale of the experiment.[29] Primary factors that affect the efficiency of the secondary metathetical isomerizations include the activity of the propagating ruthenium species and the catalyst decomposition rates. Thus, the more stable and more reactive second-

Scheme 13. Ring-Closing Metathesis of Diene 74 in the Total Synthesis of (−)-Salicylihalamide A (Snider and Song)

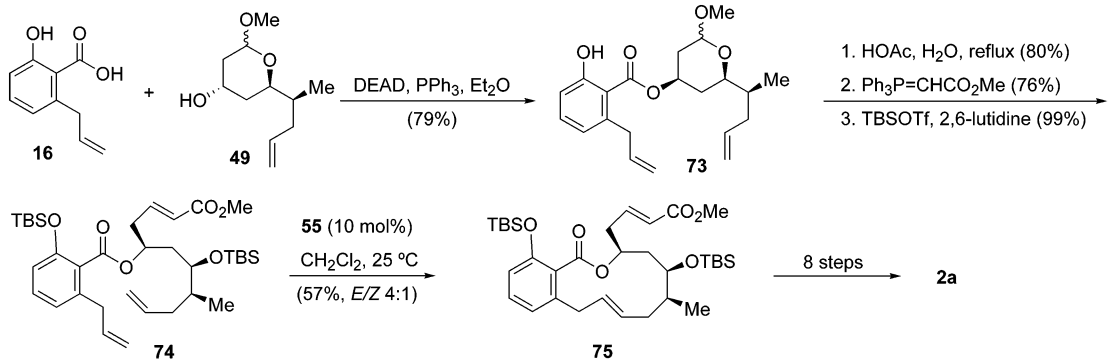

Scheme 14. Ring-Closing Metathesis of Diene 77 in the Synthesis of the Macrolactone Core of (+)-Salicylihalamide A (Georg and Co-workers)

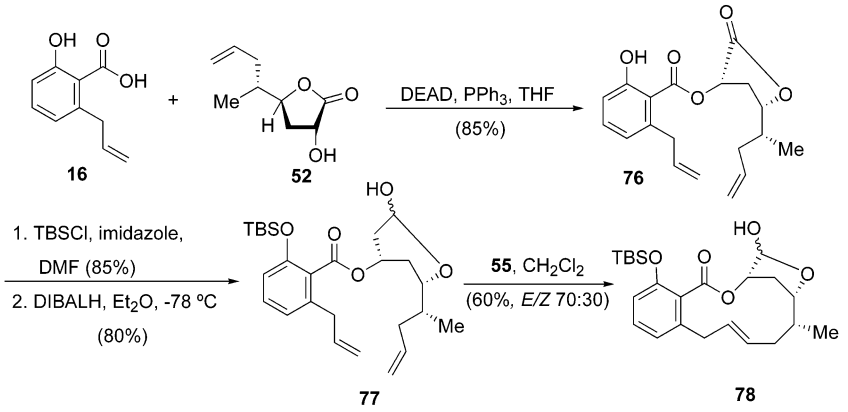

Table 1. Ring-Closing Metathesis of Diene Precursors with Ruthenium Catalysts

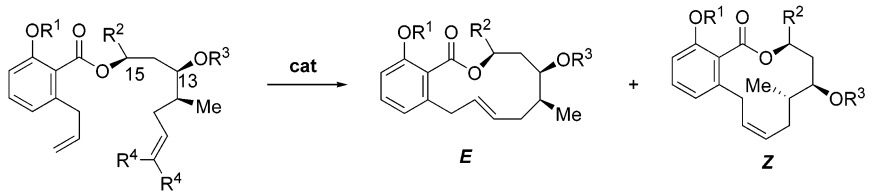

entry	substrate	R^1	R^2	R^3	R^4	catalyst	yield (%)	*E*/*Z*
1	**54a**	Me	CH_2CH_2OPMB	MOM	H	**55**	>93	88:12
2	**54a**	Me	CH_2CH_2OPMB	MOM	H	**56**	>93	68:32
3	**54b**	MOM	CH_2CH_2OPMB	MOM	H	**55**	>93	88:12
4	**54b**	MOM	CH_2CH_2OPMB	MOM	H	**56**	>93	67:33
5	**61a**	H	CH_2CH_2OPMB	MOM	Me	**57**	69	0:100
6	**61b**	TBS	CH_2CH_2OPMB	MOM	Me	**57**	91	40:60
7	**61c**	Me	CH_2CH_2OPMB	MOM	Me	**57**	93	66:34
8	**61d**	MOM	CH_2CH_2OPMB	MOM	Me	**57**	91	68:32
9	**74**	TBS	(*E*)-$CH_2CH{=}CHCO_2Me$	TBS	H	**55**	57	80:20
10	**65**	Me	(*E*)-$CH_2CH{=}CHCH_2OPMB$	TBS	H	**55**	85	91:9

generation ruthenium catalyst **56** and **57** were shown to enrich initially formed products to the thermodynamic ring closure products. De Brabander found that catalyst **56** produced a thermodynamic ratio of products on a time scale that consumed all the starting material based on the following observations (entries 2 and 4).[19] The product *E*/*Z* ratio did not change after prolonged exposure of the reaction, indicating that the equilibrium mixture was established and exposure of either geometrically pure (*E*) or (*Z*) product to catalyst **56** provided an identical 68:32 mixture of product formed. In contrast, with the first-generation ruthenium catalyst **55**, the products of the cyclization reaction afforded kinetic product ratios of higher *E*/*Z* selectivities (entries 1, 3, 9, and 10) due to their shorter lifetimes and thermal instabilities. Ruthenium catalyst **55** kinetically induced the formation of the desired (*E*)-isomers and a thermodynamic product ratio was never reached, even after prolonged reaction times. Whatever the *E*/*Z* ratios of the outcome of the RCM reactions, the isomers usually are readily separated by silica gel chromatography and do not pose major problems toward the syntheses of either **2a** or **2b**.

Scheme 15. Synthesis of the Salicylic Acid Vinyl Iodide Precursor 80 (Maier and Bauer)

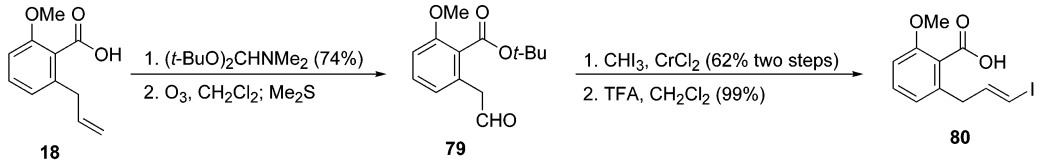

Scheme 16. Synthesis of the Diastereomerically Pure Alcohol Precursor 88 (Maier and Bauer)

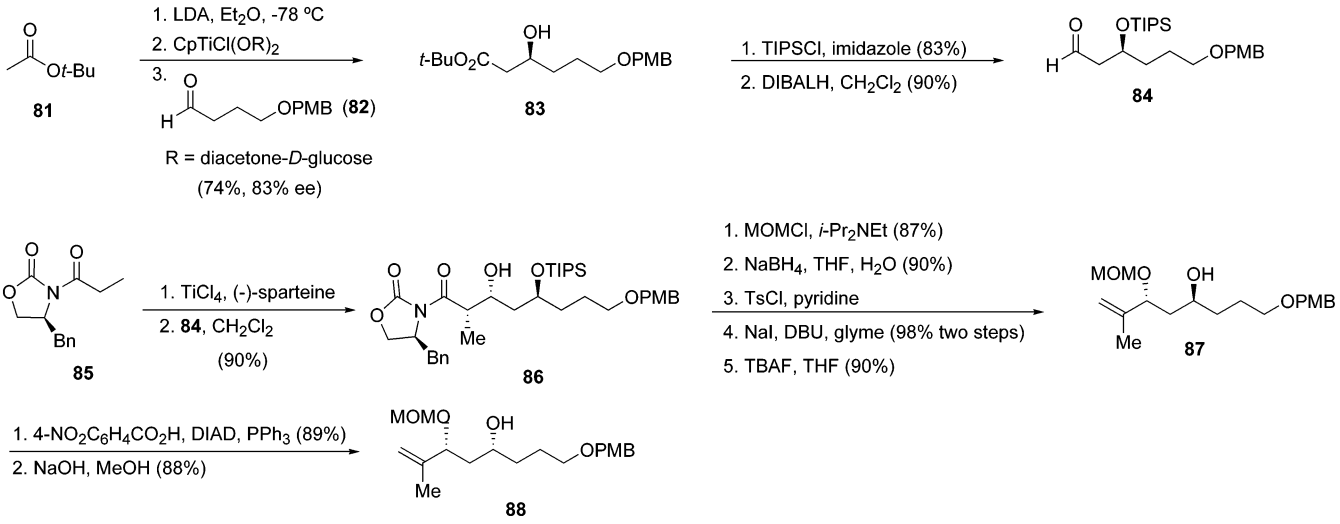

Scheme 17. Intramolecular Suzuki Coupling of Vinyl Iodide 89 To Provide the Benzolactone Core of (−)-Salicylihalamide A (Maier and Bauer)

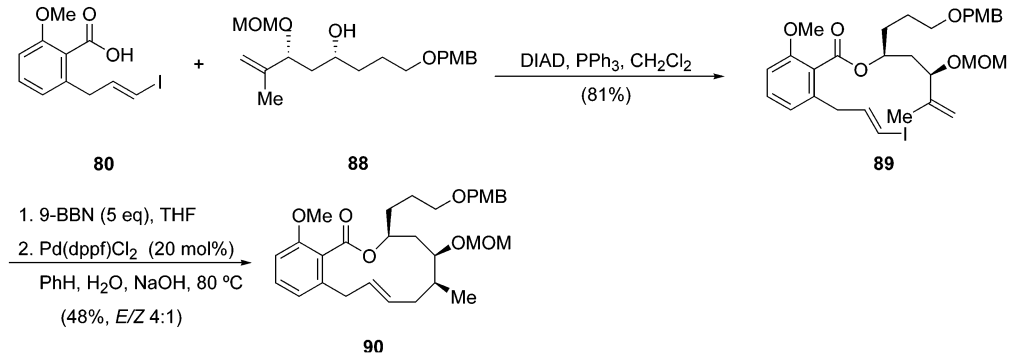

2.2. The Suzuki Coupling Approach

A synthesis of the salicylihalamide macrolactone core has been published using the intramolecular Suzuki coupling protocol. Maier and Bauer have utilized an intramolecular Suzuki coupling to establish the core structure of the macrocyclic benzolactone.[30] Esterification of salicylic acid **18** with dimethylformamide-di-*tert*-butyl acetal, followed by reductive ozonolysis, gave aldehyde **79** (Scheme 15). Subsequent Takai reaction of **79** and ester deprotection with trifluoroacetic acid furnished salicylic acid **80**.

The enantiomerically pure alcohol **88** was prepared in a multistep sequence outlined in Scheme 16. Duthaler aldol reaction[31] between aldehyde **82** and *tert*-butyl acetate (**81**) furnished the 3-hydroxy ester **83** in good yield with 83% ee (Scheme 16). Protection of the secondary alcohol of **83** with triisopropylsilyl chloride, followed by DIBALH reduction, provided aldehyde **84**. Evans aldol condensation with chiral propionate **85** and aldehyde **84** gave the *syn*-aldol product **86**. Protection of the secondary alcohol of **86**, reductive removal of the chiral auxiliary, tosylation of the primary alcohol, elimination in the presence of sodium iodide and DBU, and silyl deprotection provided the 1,1-disubstituted alkene **87** in excellent yield. Alcohol inversion of **87** was accomplished under Mitsunobu conditions with *p*-nitrobenzoic acid, followed by basic hydrolysis, to give alcohol **88**.

Thus, esterification of salicylic acid **80** with alcohol **88** under Mitsunobu conditions afforded the cyclization substrate **89** in good yield (Scheme 17). Diastereoselective hydroboration of **89**, followed by an intramolecular Suzuki coupling in refluxing benzene, yielded macrolactone **90** in a 4:1 *E*/*Z* ratio.

2.3. The Stille Coupling/Macrolactonization Approach

Rizzacasa and co-workers employed a Stille coupling/macrolactonization approach to the unsaturated benzolactone core of the salicylihalamide A in a formal total synthesis.[32] Ozonolysis/reductive workup

Scheme 18. Synthesis of the Vinylstannane Precursor 93 (Rizzacasa and Co-workers)

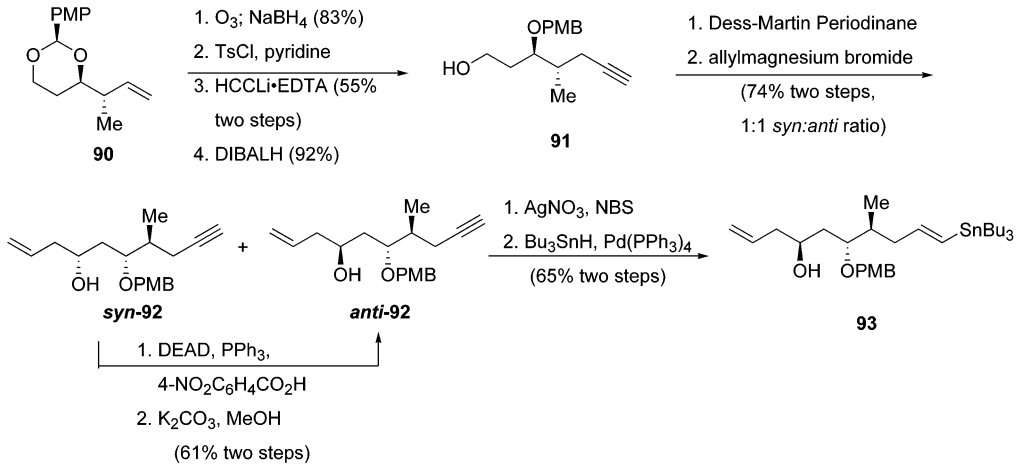

Scheme 19. Intermolecular Stille Coupling of Vinylstannane 93 with Bromoacetonide 95 To Provide the Benzolactone Core of the Salicylihalamides (Rizzacasa and Co-workers)

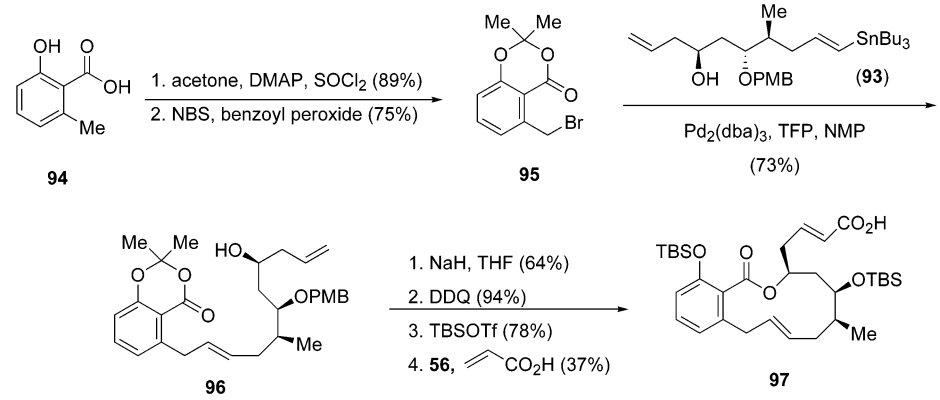

of the known optically pure acetal **90**,[33] followed by sequential tosylation, lithium acetylide addition, and DIBALH reduction of the acetal functionality, provided alcohol **91** (Scheme 18). Dess−Martin oxidation of alcohol **91** and addition of allylmagnesium bromide afforded a ~1:1 ratio of *syn*-**92** and *anti*-**92**, which were easily separated by silica gel chromatography. The undesired alcohol could be converted to the desired alcohol by Mitsunobu inversion. *Anti*-**92** is then converted regioselectively to vinyl stannane **93**.

Stille coupling between vinyl stannane **93** and bromoacetonide **95**, prepared in two steps from 6-methylsalicylic acid (**94**), under Farina conditions afforded the (*E*)-alkene **96** in excellent yield (Scheme 19). Crucial macrolactonization was effected by treatment of a dilute solution of **96** with sodium hydride, which provided the intermediate benzolactone in reasonable yield; subsequent PMB deprotection, TBS reprotection, and Grubbs's cross-metathesis with second-generation ruthenium catalyst **56** and acrylic acid gave the α,*β*-unsaturated acid **97**. Acid **97** was a common intermediate used for De Brabander's[19a] and Smith's[23] syntheses of salicylihalamide A (**2a**), thus constituting a formal total synthesis.

3. Chemistry of Apicularen A

3.1. The De Brabander Synthesis

Apicularen A (**3**) differs from the other benzolactone enamide natural products in that it contains a pyran ring, probably formed biosynthetically through a transannular cyclization. There are only two total and one formal total syntheses of apicularen A (**3**) reported so far. De Brabander and co-workers reported the first enantioselective total synthesis of apicularen A (**3**).[34,35] Hetero-Diels−Alder enantioselective reaction of Danishefsky's diene **99** and aldehyde **98** with Jacobsen's chiral chromium(III) complex **100** afforded dihydropyranone **101** in 84% ee (>99% ee after recrystallization) after treatment of the intermediate cycloadduct with trifluoroacetic acid (Scheme 20).[34] Copper(I)-catalyzed conjugate addition of vinylmagnesium bromide to dihydropyranone **101** gave diastereomerically pure 1,6-*trans*-tetrahydropyranone **102**. Sequential attempted stereoselective ketone reduction, silylation, hydroboration, and oxidation of tetrahydropyranone **102** provided aldehyde **103** as an inseparable mixture of epimeric alcohols in a 1:1 ratio. Reagent-controlled allylation of aldehyde **103** either with Brown's *β*-allyldiisopinocampheylborane or with titanium tetrachloride and allyltrimethylsilane delivered an identical 77:23 mixture of diastereomeric homoallylic alcohols **104** and **105** in a mismatched double-diastereodifferentiating reaction. A solution of homoallyl alcohol **104** (mixture of C-11 epimers) in the presence of sodium hydride effected the crucial lactonization step to give phenol **106**.

Phenol **106** was elaborated to geometrically pure (*E*)-allyl ester **107** by oxidative cleavage of the

Scheme 20. Synthesis of Phenolic Ester 106 (De Brabander and Co-workers)

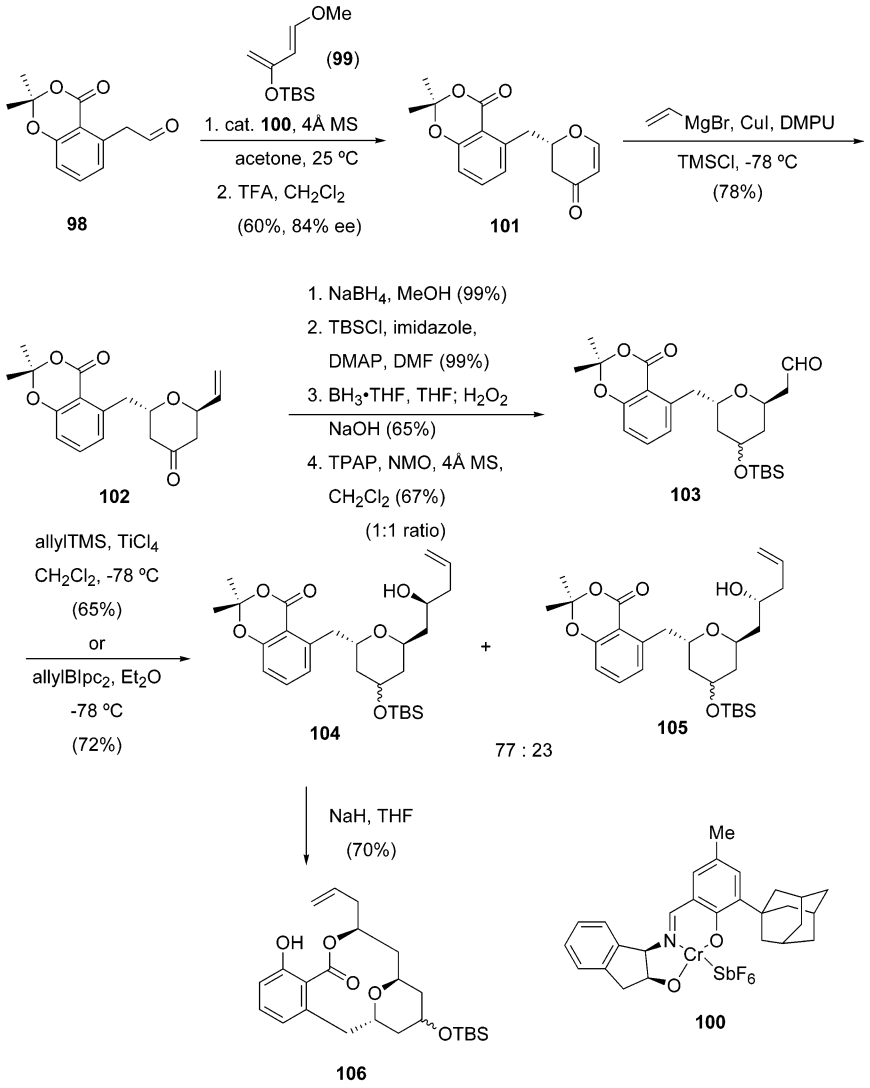

terminal olefin and homologation of the resulting aldehyde with allyldiethylphosphonoacetate (Scheme 21).[35] Palladium-catalyzed deprotection of **107**, followed by chromatographic separation of the C-11 epimers, afforded pure carboxylic acids **108** and **109**. These acids were separately transformed to intermediate isocyanates and reacted with lithiated 1,3-hexadiene (1:1 *E*/*Z* isomers) to give **110**, **111**, **112**, and apicularen A (**3**).

3.2. The Taylor Formal Synthesis

Taylor and co-workers have also synthesized phenol **106** from D-glucal in a formal total synthesis of apicularen A (**3**, Scheme 22).[36] D-Glucal (**113**) was sequentially derivatized to thiocarbonyl imidazole **114**, which underwent tributyltin hydride-mediated deoxygenation, acid-catalyzed addition of methanol with concomitant deprotection of the primary silyloxy group, and trifylation to triflate **115**. Benzofuryl Grignard reagent **116**, the most effective salicylate equivalent for the triflate displacement process, was allowed to react with triflate **115** in a copper(I) bromide-catalyzed procedure to give coupled product **117**. Adduct **117** was oxidatively cleaved with ozone to aldehyde **118**, which was then converted to methyl ester **119** via standard procedures. Lewis acid-mediated allylation of the anomeric methyl acetal and reprotection of the cleaved TPS group to the TBS group afforded alkene **120**. Ozonolysis of alkene **121**, followed by Brown's allylation, delivered an inseparable 9:1 ratio of diastereomeric alcohols. Lithium iodide-induced ester cleavage, Keck macrocyclization, and deprotection with 9-iodo-9-BBN provided phenol **106**.

3.3. The Nicolaou Synthesis

Nicolaou and co-workers recently published a total synthesis of apicularen A (**3**) and its $\Delta^{17,18}$-(*Z*)-isomer.[37] The group developed five reiterations of the allylation−ozonolysis sequence as the key steps to "mimic" nature's polyacetate biosynthetic pathway. Thus, acetonide triflate **15** was coupled with allyltributyltin under palladium catalysis, followed by ozonolysis to the intermediate aldehyde, stereoselective allylation with Brown's (−)-*β*-allyldiisopinocampheylborane, protection, and ozonolysis, to give the aldehyde **122** (Scheme 23). Allylation of aldehyde **122** this time with the (+)-enantiomer of Brown's reagent ((+)-Ipc$_2$Ballyl), followed by mild acidic treatment, furnished the intermediate diol, which on ozonolysis gave aldehyde which spontaneously cyclized to the lactol, and acetylation provided the diacetate **123** as

Scheme 21. Elaboration of Phenolic Ester 106 to Apicularen A (De Brabander and Co-workers)

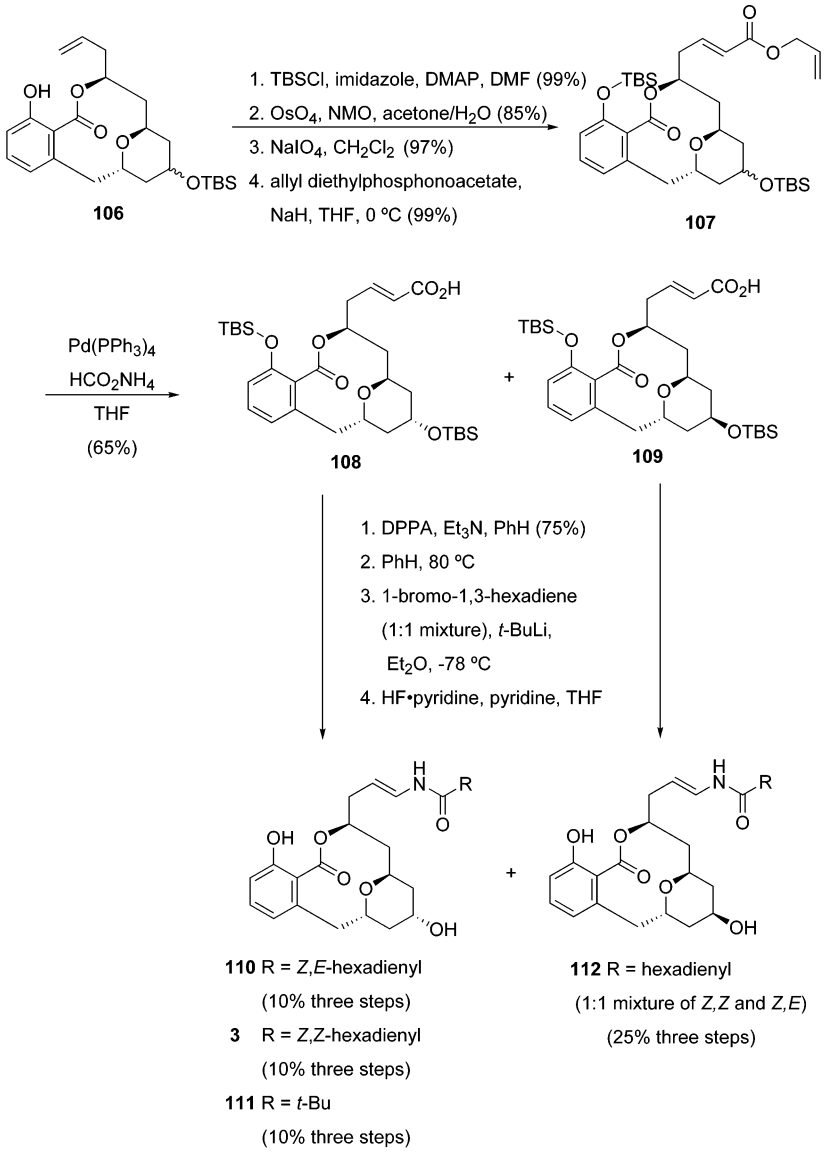

a mixture of anomers (α: β ca. 3:1). Anomeric allylation of **123** with allyltrimethylsilane in the presence of boron trifluoride etherate led stereoselectively to the intermediate allyl derivative with the desired anti stereochemistry. Another ozonolysis−allylation sequence employing (+)-Ipc_2B (allyl) provided the homoallyl alcohol **124** in >90% de. Sequential silylation of homoallyl alcohol **124**, ozonolysis, and Takai iodoolefination furnished (*E*)-vinyliodide **125** contaminated with ca. 10% of its (*Z*)-isomer. This mixture was coupled with the primary amide **64** in the presence of copper(I) thiophene carboxylate (CuTC) and rubidinium carbonate to give stereospecifically the $\Delta^{17,18}$-(*E*)-enamide derivative **126** with its (*Z*)-isomer (based on 50% conversion, ca. 10:1 ratio). The two isomers were chromatographically separated, and each underwent silyl deprotection and base-induced cyclization to give apicularen A (**3**) and its isomer.

3.4. The Rizzacasa Approach

Rizzacasa and co-workers reported a synthesis of the core of apicularen A (**3**) by a novel transannular conjugate addition.[38] The racemic bis-silyl ether **127**[39] was transformed into alkyne **128** via ozonolysis and lithium acetylide addition, followed by separation of the diastereomers (Scheme 24). Silyl group manipulations and palladium-catalyzed hydrostannylation afforded vinyl stannane **129**, which was then Stille cross-coupled with bromide **130** to give alkene **131**. Novel base-induced macrolactonization, methylation of the resultant phenoxide ion, desilylation, and allylic oxidation then yielded enone **132**. Acid treatment of **132** under thermodynamic condition gave pyranones **133** and **134** in a 9:1 trans:cis ratio. The authors noted that these results do not confirm this mode of cyclization as biomimetic; they recognize that this facile cyclization of **132** provided support to this proposal.

3.5. The Maier Approach

A biomimetic strategy was applied by Maier and Kuhnert in a laboratory setting to demonstrate the feasibility of this approach on a model intermediate.[40] The triflate precursor **137** is prepared in several steps, as shown in Scheme 25. Subjecting methoxy-

Scheme 22. Formal Total Synthesis of Apicularen A with Phenolic Ester 106 (Taylor and Co-workers)

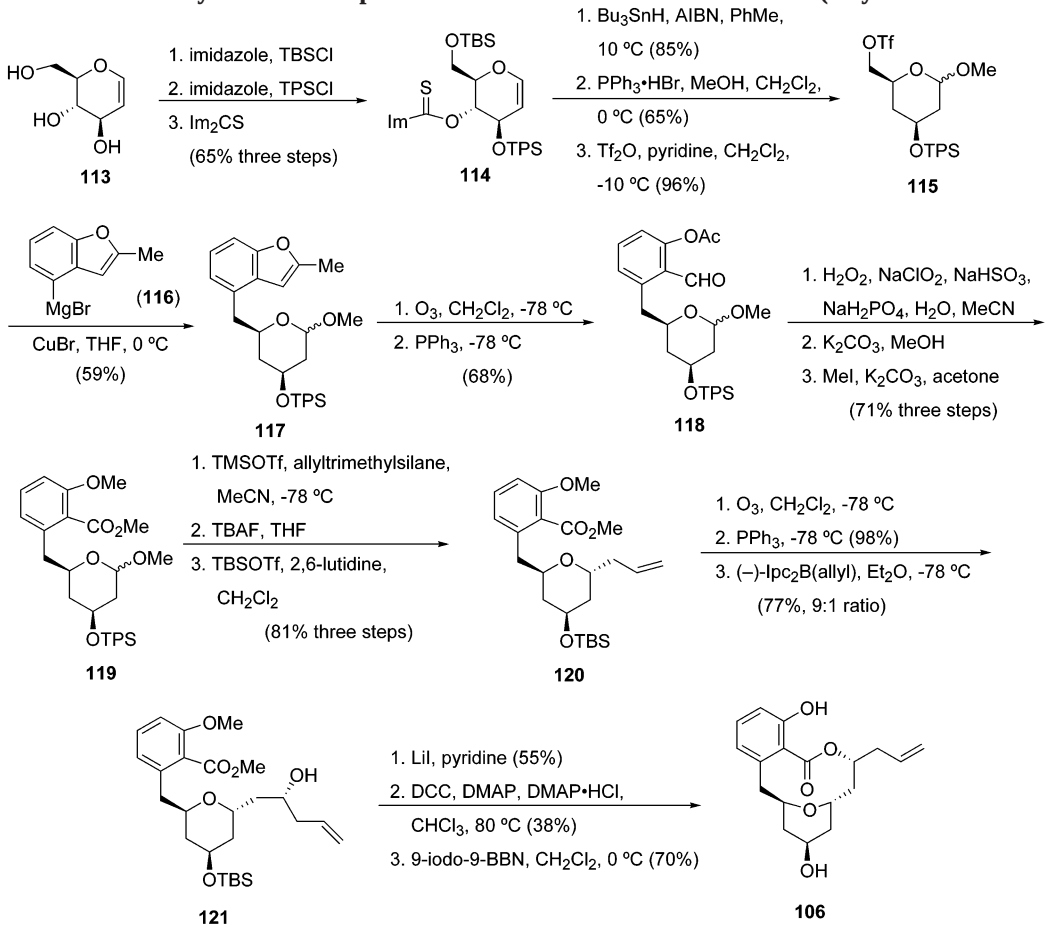

Scheme 23. Total Synthesis of Apicularen A via Repetitive Allylation/Ozonolysis Sequence (Nicolaou and Co-workers)

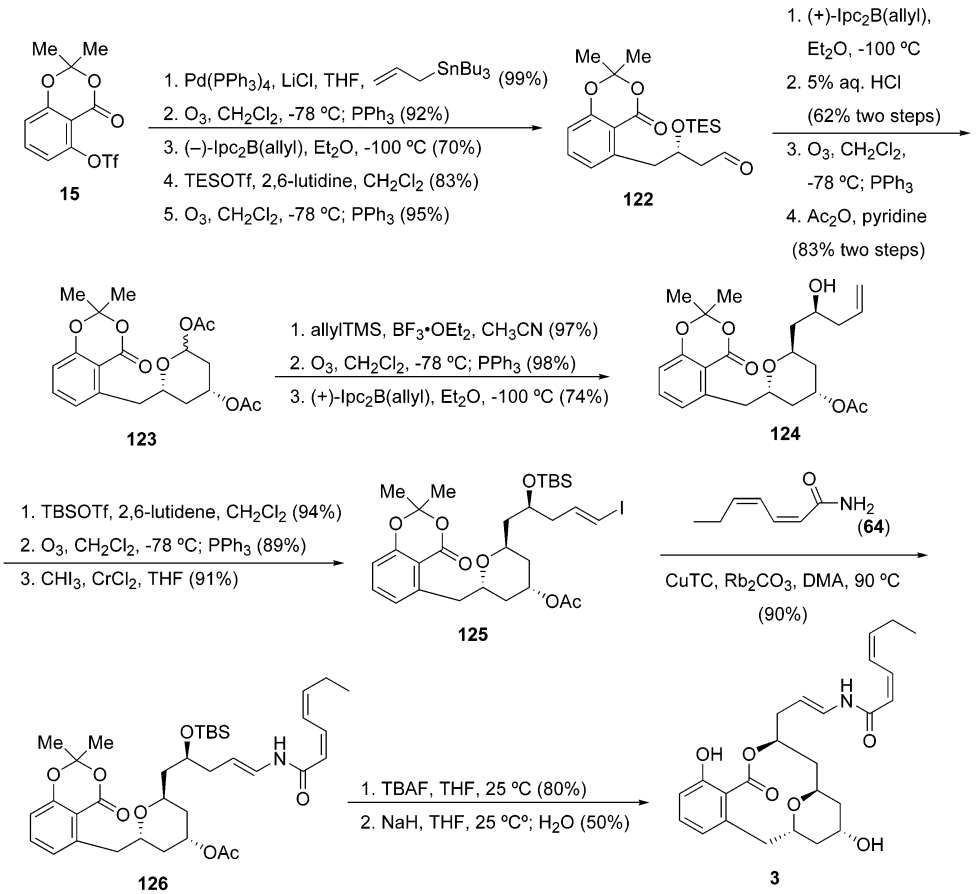

Scheme 24. Synthesis of the Core of Apicularen A by Novel Transannular Conjugate Addition of Lactone 132 (Rizzacasa and Co-workers)

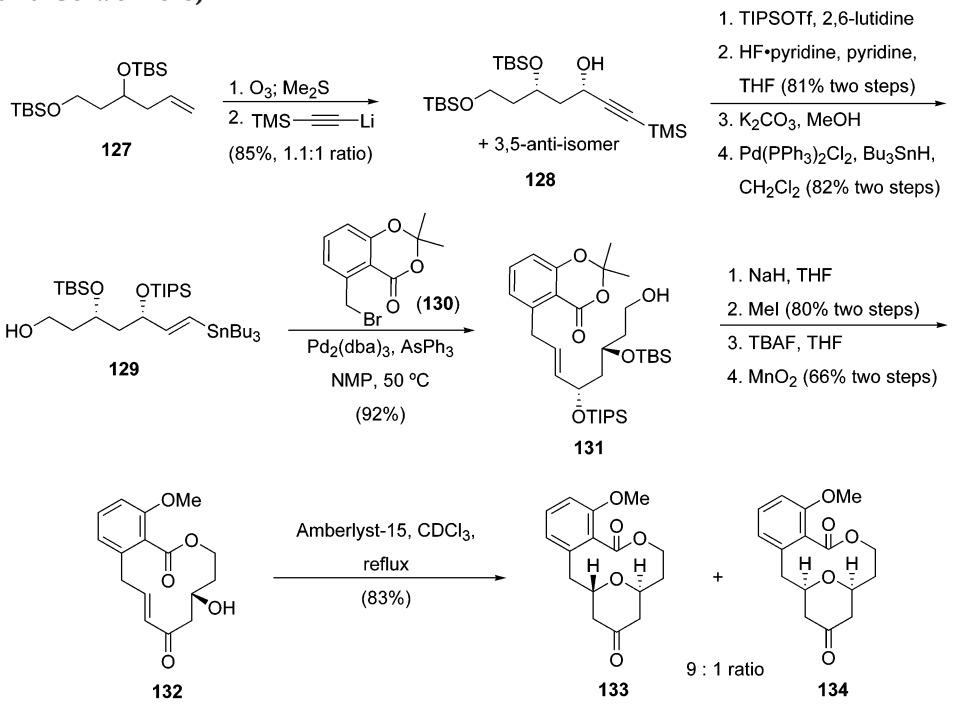

Scheme 25. Synthesis of Salicylic Triflate 137 (Maier and Kuhnert)

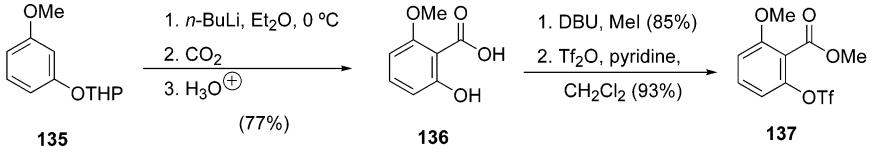

benzene **135** to metalation conditions and quenching with carbon dioxide provided salicylic acid **136**, which was then esterified and triflated to give precursor **137**.

Vinyl stannane **144** is synthesized according to the route outlined in Scheme 26. Triol **138**, available from D-glutamic acid,[41] in a series of steps involving acetonide protection, benzylation, acetonide removal, and Sharpless epoxide formation, yielded enantiomerically pure epoxide **139**. Alkylation of dithiane **140** with epoxide **139** took place in the presence of *tert*-butyllithium and tetramethylethylenediamine (TMEDA) to provide alcohol **141** in good yield. Hydrolysis of the dithiane group required the combination of mercury(II) perchlorate in the presence of Hünig's base to give the diol **142**, in which the cleavage of the triethylsilyl ether was also noticed. Diol **142** was diastereomerically reduced and protected to acetonide **143**, which was then extended to the intermediate alkyne via the mesylate and the iodide. The intermediate alkyne was coverted via hydrostannylation to the vinyl stannane **144**.

Stille cross-coupling of vinyl stannane **144** with triflate **137** furnished styrene **145** (Scheme 27). Acetal deprotection and acid hydrolysis of styrene **145** provided diol **146**, which under Yamaguchi macrolactonization conditions afforded benzolactone **147**. Pyran formation was realized with *N*-phenylselenophthalimide (*N*-PSP) in the presence of chlorosulfonic acid (CSA) to give selenide **148**. Reductive removal of the phenylselenyl group with tributyltin hydride gave compound **149**.

Scheme 26. Synthesis of Vinylstannane 144 (Maier and Kuhnert)

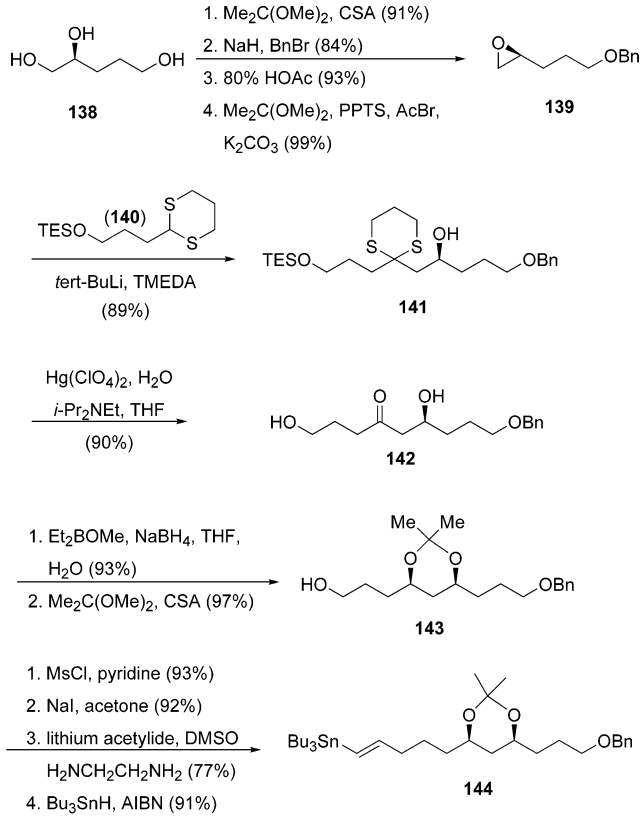

Scheme 27. Synthesis of the Core Structure of Apicularen A by Transannular Cyclization of Macrolactone 147 with *N*-Phenyl Selenophthalimide (*N*-PSP) and Chlorosulfonic Acid (CSA) (Maier and Kuhnert)

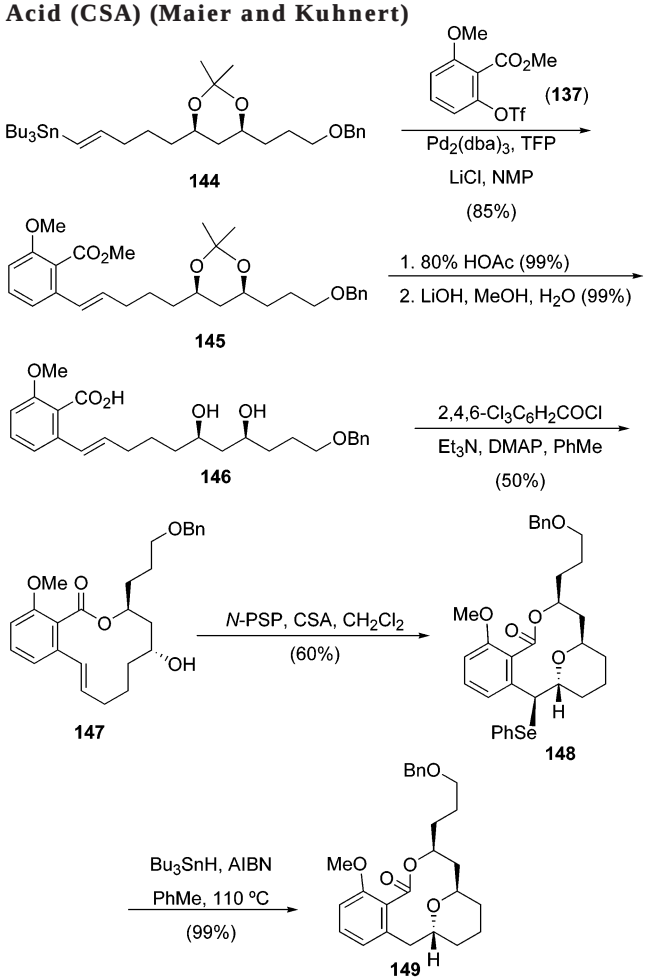

4. Chemistry of Lobatamide C

Porco and co-workers have reported the only total synthesis of lobatamide C (**4b**).[42] The synthesis of the enamide fragment **155** began with (*R*)-ethyl-3,4-epoxybutanoate (**150**). Addition of the acetylenic alane reagent derived from trimethylsilyl acetylene to **150**, followed by silyl protection and silver-induced bromination, provided bromoalkyne **151** (Scheme 28). Palladium-catalyzed hydrostannylation of **151** and iodine exchange furnished vinyl iodide **152**. Copper(I) thiophenecarboxylate (CuTC)-mediated vinylic substitution of **152** with (*E*)-*O*-methyloxime amide **153** with base and additives then led to a 45% yield of enamide **154**, along with 10% of the easily separable (*Z*)-oxime stereisomer. Desilylation and lithium hydroxide hydrolysis provided the labile enamide acid fragment **155**.

Benzyl bromide **156** was prepared from aryl triflate **15** (Scheme 29). Sequential treatment of **15** in the presence of lithium dimethylcuprate, hydrolysis, carboxylate alkylation, silyl protection, and benzylic bromination gave benzyl bromide **156**. (*S*)-3-Butyn-2-ol (**157**) underwent silyl protection, zirconocene−zinc transmetalation, and addition to enal **158** in the presence of thiol ligand **159**, silyl protection, and lithiation−trimethylstannylation to afford vinyl stannane **160** (Scheme 30). Benzyl bromide **156** was then palladium-catalyzed cross-coupled with vinyl stannane **160** and selectively deprotected to give salicylate cyanomethyl ester **161**.

Scheme 29. Synthesis of Benzyl Bromide 156 (Porco and Co-workers)

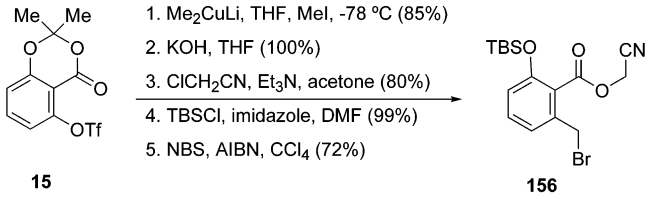

The tetrabutylammonium salt of enamide **155** participated in an efficient esterification reaction with salicylate cyanomethyl ester **161** to provide the desired salicylate epimers **162** (Scheme 31). Treatment of **162** with HF−pyridine afforded the intermediate hydroxy acids, which gratifyingly underwent smooth macrolactonization under Mitsunobu conditions. The resulting TBS-protected lactones were separated by flash column chromatography, and each was deprotected separately with HF−pyridine to give lobatamide C (**4b**) and its C15 epimer.

It should be noted that a sensitive *N*-acyl enamine side chain is usually installed at the end of the synthesis. There have been several recent synthetic methodology publications relating to the preparations of these unusual, highly unsaturated *N*-acyl enamine side chains.[43] A few comments should be noted on the different approaches of the enamide side-chain installation in several of the total syntheses of salicylihalamide A (**2a**). Additions of lithiodienes to isocyanates, as seen in De Brabander's route (Scheme 9) or Snider's route (Scheme 13), cross-coupling of

Scheme 28. Synthesis of Enamide Fragment 155 (Porco and Co-workers)

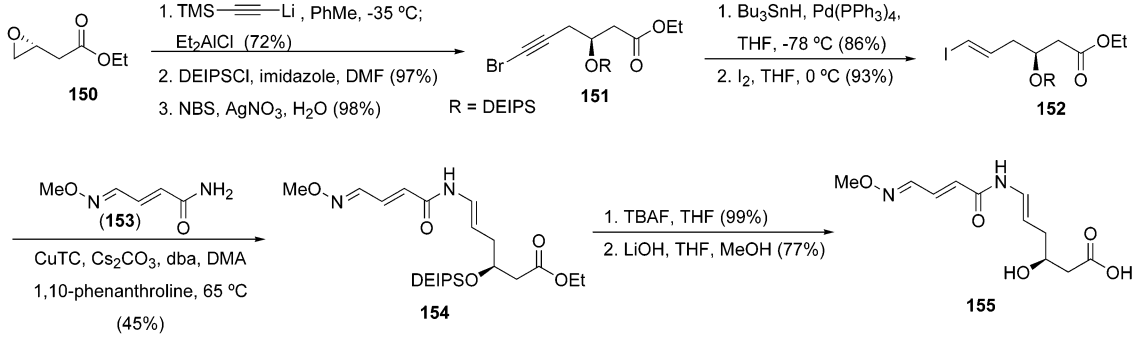

Scheme 30. Synthesis of Salicylic Cyanomethyl Ester 161 (Porco and Co-workers)

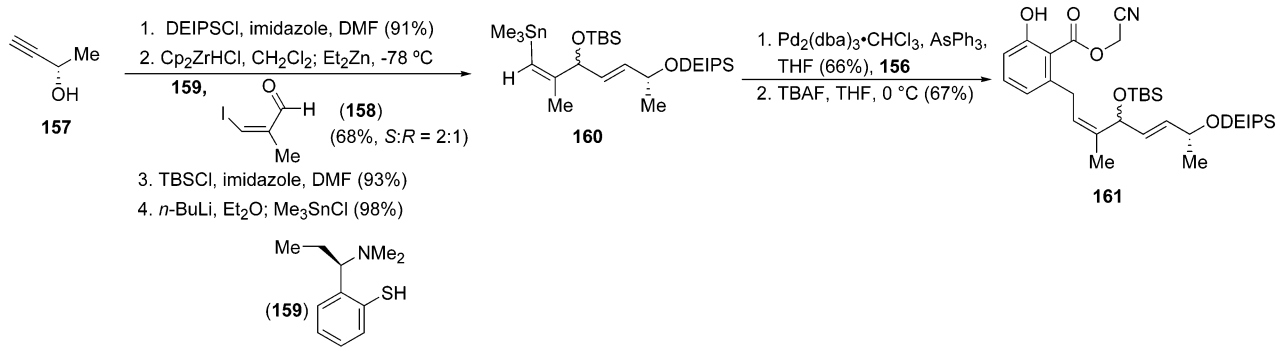

Scheme 31. Macrocyclization of Acid 162 under Mitsunobu Conditions in the Total Synthesis of Salicylate Antitumor Macrolide Lobatamide C (Porco and Co-workers)

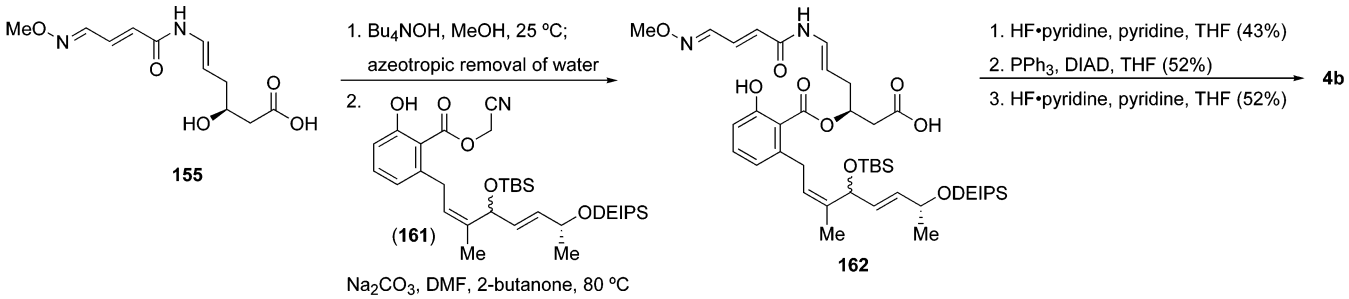

vinyl iodide with dienyl amide in Furstner's route (Scheme 10), and base-promoted elimination of *N*,*N*′-bis-acylated aminal in Labrecque's synthesis all give *E*/*Z* isomers of the enamide side-chain products, which usually are separated by preparative high-pressure liquid chromatography. On the other hand, Smith performed the acylation of a dienyl acid chloride to an enaminocarbamate (Scheme 11) to give a product that was essentially the (*Z*,*Z*)-isomer.

5. Chemistry of the Oximidines

5.1. The Coleman Approach

Coleman and Garg developed a stereocontrolled construction of a series of 12-membered diene and triene lactones, which are characteristic of the core of antitumor agent oximidine I (**6a**) and oximidine II (**6b**).[44] Modified Castro−Stephens cyclization of alkyne **163** afforded cyclic enyne **164**, which was stereoselectively reduced with zinc metal and copper(I) bromide in the presence of 1,2-dibromoethane to provide (*E*,*Z*)-diene lactone **165** (Scheme 32). Similarly, cyclic enyne **168** was prepared from alkyne **166**. Cyclic enyne **164** and (*E*,*Z*)-diene lactone **165** could also be prepared from enyne **169** and diene **170**, respectively, using the Mitsunobu protocol.

5.2. The Maier Approach

Maier and Scheufler utilized a Stille/macrocyclization approach to the synthesis of the oximidine core.[45] 6-Heptynoic acid (**171**) was converted to allylic PMB-protected ether **172** in a five-step procedure, involving reduction, Swern oxidation, Wittig homologation, allyic alcohol formation, and protection (Scheme 33). Sharpless asymmetric dihydroxylation with AD-mix α provided diol **173** in 95% enantioselectivity. Tributyltin hydride-mediated hydrostannylation provided vinyl stannane **174** as the major product. Performing this reaction under palladium-catalyzed conditions gave a 62:38 ratio of **174**:**175**.

Stille cross-coupling of vinyl stannane **174** with triflate **137** provided styrene **176** (Scheme 34). Acetal deprotection and base hydrolysis of styrene **176** provided diol **177**, which under Yamaguchi macrolactonization conditions afforded benzolactones **178** and **179** in a 60:40 ratio.

5.3. The Porco Synthesis

Porco and Wang reported the first total synthesis of oximidine II (**3b**) employing a ring-closing metathesis of a well-defined bis-diene substrate to construct the unusual macrocyclic triene core, and a stereoselective copper-mediated amidation of a (*Z*)-vinyl iodide to construct the enamide side chain.[46] Asymmetric Brown allylboration of aldehyde **180** afforded alcohol **181** as a single diastereomer (Scheme 35). Alcohol **181** was converted in five steps to cis-diene **182**. Homologation of (*E*)-crotonaldehyde (**183**) and coupling with triflate **15** under palladium-catalyzed conditions gave (*E*,*E*)-diene **184**. Treatment of the anion of **182**, followed by addition of **184** and silylation, provided the bis-diene **185** in a one-pot procedure. Ring-closing metathesis of bis-diene **185** with Grubbs's second-generation catalyst **56** furnished the oximidine II core **186** in moderate yield, accompanied by oligomeric byproducts. PMB deprotection, alcohol oxidation, and Wittig olefination of **186** afforded **187** as a single olefin isomer, which was then MOM-deprotected and silylated to afford (*Z*)-vinyl iodide **188**. Finally, amidation of **188** with copper(II) thiophene carboxylate in the presence of ligand and base, followed by deprotection, gave oximidine II (**3b**).

Scheme 32. Stereocontrolled Synthesis of Diene and Triene Macrolactones 164, 165, and 168 of the Oximidines by Intramolecular Castro−Stephens Coupling or by Mitsunobu Coupling (Coleman and Garg)

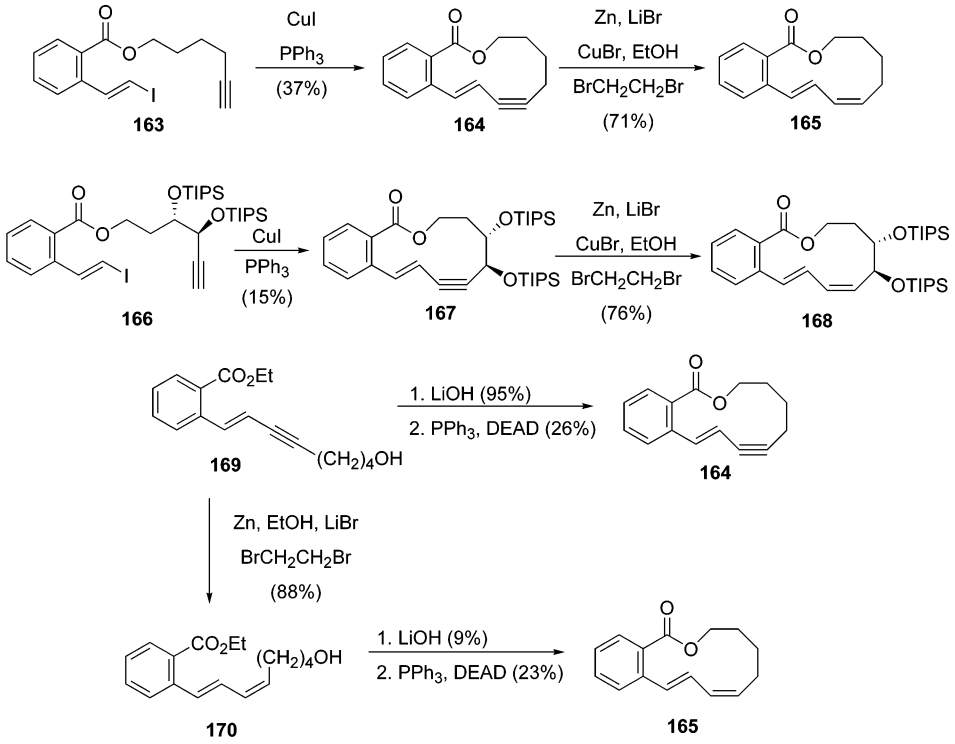

Scheme 33. Synthesis of Vinylstannane 174 (Maier and Scheufler)

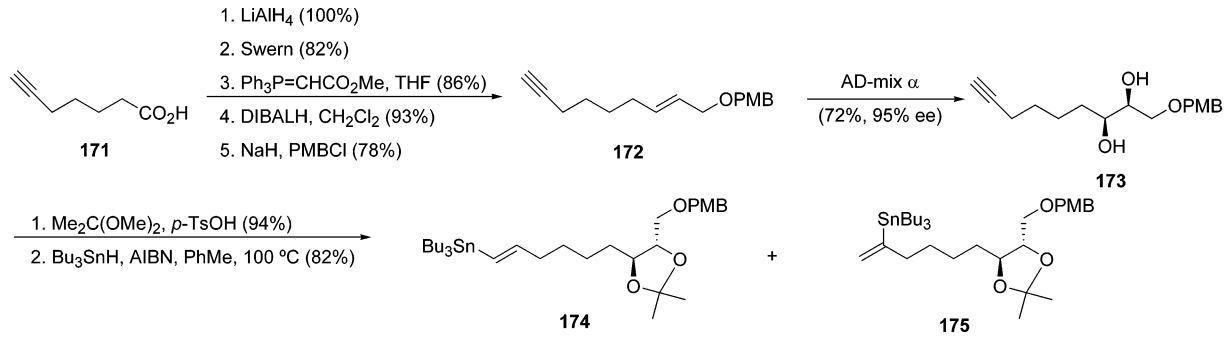

6. Biology of the Salicylihalamides and Their Modified Congeners

Boyd has described the origin, concept, rationale, and technical details of the NCI 60-cell line screen, along with the research applications such as the COMPARE algorithm.[47] Since the initial discovery of the structures of (−)−salicylihalamide A (**2a**) and lobatamide A (**4a**), both compounds were tested in the NCI 60 cell line human tumor screen, and both compounds were found to give a striking pattern of differential cytotoxicity (Table 2). This screen provided a powerful new tool to assess whether new compounds have the same, similar, or different mechanisms of antitumor action relative to the profiles of reference antitumor compounds contained in the NCI's standard agent database. The testing of bafilomycin A_1 (**190**, Figure 4), salicylihalamide A (**2a**), lobatamide A (**4a**), and oximidine II (**6b**) gave essentially identical 60-cell tumor screening profiles, with the leukemia and melanoma cell lines having the greatest sensitivity as a whole (Figure 5). From these screens, Boyd has suggested that these four compounds may act by a novel mechanism of action, since their activity profile did not match compounds whose mechanisms of action are known using the COMPARE algorithm.

The Vacuolar ATPase (V-ATPase) enzyme has been identified as the putative target of (−)-salicylihalamide A (**2a**).[48] V-ATPases are ubiquitous proton-translocating pumps of eukaryotic cells, which reside within many intracellular compartments, such as endosomes, lysosomes, and secretory vesicles, which serve as crucial transporters responsible for the regulation of pH.[48] The pumps are oriented such that protons are pumped out of the cytoplasm into the organelle or the extracellular space, where the hydrolysis of adenosine triphosphate (ATP) generates an electrochemical potential across the membrane that drives the transport of ions and solutes (Figure 6). V-ATPases have diverse functional roles such as receptor-mediated endocytosis, intracellular targeting of lysosomal enzymes, protein processing and degradation, and transport of small molecules. V-ATPases can also be found in the plasma membrane of

Scheme 34. Model Macrocyclization of Acid Diol 177 to the Macrocyclic Subunit of the Oximidines (Maier and Scheufler)

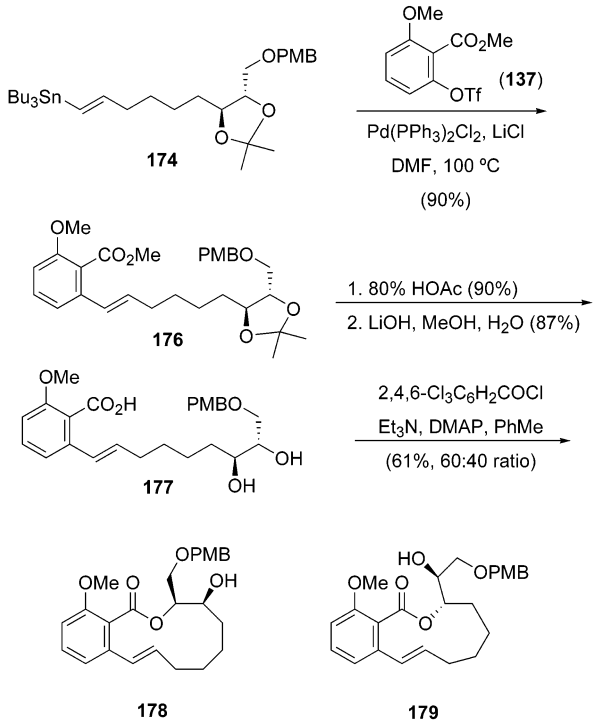

certain cells, such as renal-intercalated cells for acid secretion, osteoclasts for bone degradation, and macrophages for control of cytoplasmic pH.

The most remarkable feature of V-ATPases is the great diversity of functions that they serve in eukaryotic organisms, and this enzyme system can potentially be an attractive pharmaceutical target for drug discovery research. Abnormal secretion of degradative enzymes, diabetes, cardiovascular and clotting disorders, Alzheimer's disease, disorders involving abnormal receptor-mediated uptake processes, glaucoma, defective urinary acidification, osteoporosis, and cancer are diseases which have been implicated in defective V-ATPase function.[49] However, almost all drug discovery aimed at inhibition of V-ATPase-derived function has failed to date.

In contrast to bafilomycins and other prototypical V-ATPase inhibitors[50] such as concanamycin A (**191**), salicylihalamide A (**2a**) discriminates between mammalian and nonmammalian V-ATPases (Figure 4). Thus, salicylihalamide A (**2a**) and its congeners have become exciting new targets for chemical synthesis, lead optimization studies, and the preparation of designed analogues to further define structure−activity relationships (SARs) with the molecular target. De Brabander and co-workers have initiated the first SARs of the salicylihalamide analogues.[19a,51] Their initial efforts were aimed at side-chain modifications prepared from the advanced intermediate isocyanate **59** (see Scheme 9). The in vitro inhibitions of V-ATPase activity by (−)-salicylihalamide A (**2a**), its enantiomer **1a**, and synthetic derivatives (see Figure 7) are summarized in Table 3. For their studies, De Brabander and co-workers utilized a

Scheme 35. Ring-Closing Metathesis of Bis-diene 185 in the Total Synthesis of Oximidine II (Wang and Porco)

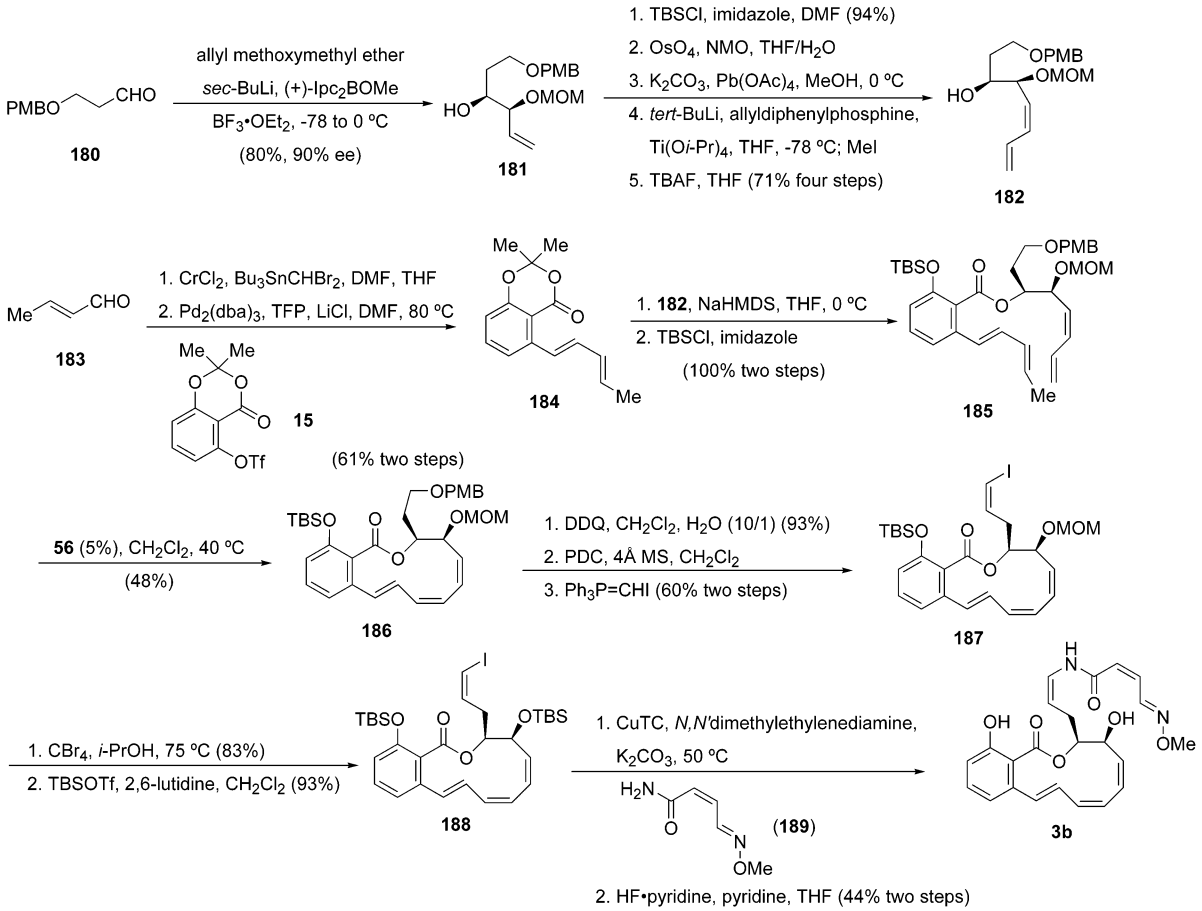

Table 2. NCI 60 Human Cell Line Screen (Averaged, Individual Negative Log GI_{50} Values Comprising the GI_{50} Mean Graph)

		−Log GI_{50}				−Log GI_{50}	
panel name	cell line name	**2a**	**4a**	panel name	cell line name	**2a**	**4a**
leukemia	CCRF-CEM	7.89	9.21	melanoma	LOX IMVI	9.11	9.70
	HL-60 (TB)	9.04	9.59		MALME-3M	7.62	8.52
	K-562	8.41	8.72		M14	8.92	9.57
	MOLT-4	7.96	9.05		SK-MEL-2	7.47	8.89
	RPMI-8226	7.89	8.89		SK-MEL-28	7.00	8.12
	SR	8.44	9.59		SK-MEL-5	9.00	9.60
non-small cell lung	A549/ATCC	8.54	9.00		UACC-257	8.47	9.11
	EKVX	7.52	8.92		UACC-62	8.38	9.32
	HOP-62	8.38	9.49	ovarian	IGR-OV1	7.89	8.60
	HOP-92	7.77	8.85		OVCAR-3	7.03	8.96
	NCI-H226	8.80	9.48		OVCAR-4	5.30	
	NCI-H23	6.55	8.36		OVCAR-5	8.11	7.51
	NCI-H322M	6.72	8.31		OVCAR-8	8.43	9.22
	NCI-H460	9.01	9.15		SK-OV-3	5.54	>7.00
	NCI-H522	7.26	8.70	renal	786-0	7.92	9.39
colon	COLO205	8.07	9.12		A498	6.55	7.42
	HCC-2998	6.74			ACHN	8.01	9.10
	HCT-116	8.74	9.11		CAKI-1	8.96	8.70
	HCT-15	8.44	8.60		RXF-393	9.07	9.68
	HT29	8.54	9.35		SN12C	7.77	7.49
	KM12	8.30	9.04		TK-10	5.74	7.59
	SW-620	7.54	8.77		UO-31	8.31	8.82
brain	SF-268	7.55	9.32	breast	MCF7	7.12	8.14
	SF-295	8.96	9.44		MCF7/ADR-RES	8.07	8.60
	SF-539	7.89	9.13		MDA-MB-231/ATCC	6.92	7.77
	SNB-19	6.47	>7.00		HS578T	5.85	8.57
	SNB-75	6.21	8.34		MDA-MB-435	7.82	9.03
	U251	7.57	9.00		MDA-N	8.00	8.80
prostate	PC-3	7.51	8.29		BT-549	9.30	9.30
	DU-145	8.26	8.27		T-47D	8.34	8.70

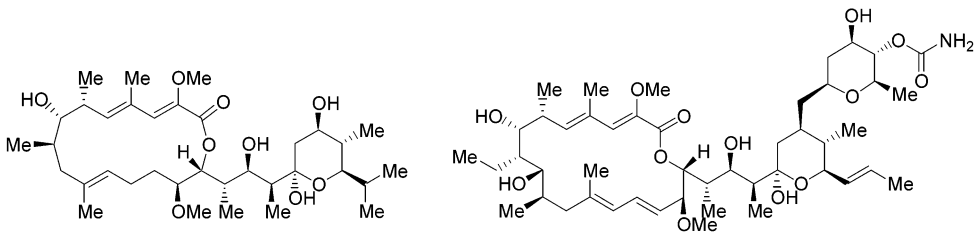

Figure 4. Structures of bafilomycin A_1 (**190**) and concanamycin A (**191**).

reconstituted, fully purified V-ATPase from bovine brain extracts to completely eliminate potential effects arising from contaminating nonvacuolar ATPase activities that were present in the crude membrane preparations utilized in the initial[5] study. It was thus demonstrated for the first time that synthetic (−)-salicylihalamide A (**2a**) inhibits ATP-energized proton pumping of the intact, reconstitutively active V-ATPase with an IC_{50} value of <1.0 nM. The unnatural enantiomer (+)-salicylihalamide A (**1a**) was 300-fold less potent (Table 3, entry 1).

Side-chain-modified analogues **196**−**200** all retain the ability to inhibit proton-pumping activity at concentrations similar to those of the parent compound. These studies showed that the hexadienoyl moiety was not crucial for biological activity and that even substantially more demanding modifications can be made without lowering biological activity, except for farnesylated analogue **201**, which showed a 1000-fold drop in activity. It is interesting to note that dimer structures **193**−**195** retained significant activity. Seriously compromised potency of allyl ester **192** and octanoate **202** in the in vitro assay emphasized the importance of the *N*-acyl enamine functionality. The *N*-carbamoyl enamine derivative **203** retained significant ability to inhibit proton pumping in the V-ATPase assay; however, the amine carbamate **204** activity was reduced 10-fold with the double bond absent. Finally, protected alcohols either at C-13 (analogue **206**) or at the phenol (analogue **205**) led to a significant drop in biological activity. Thus, this eliminated the possibility of exploiting the obvious functional core for future SAR studies.

De Brabander and co-workers also studied the growth inhibition of the SK-MEL 5 human melanoma cell line with the synthetic analogues described in Figure 7.[19a,51] The results were largely submicromolar inhibitors in vitro, as shown in Table 4. Although SARs found in this assay generally mirrored those of the in vitro V-ATPase assay, they do not necessarily indicate a link between inhibition of the vacuolar ATPase and cytotoxicity. Further studies will be necessary to clarify the biology in this area.

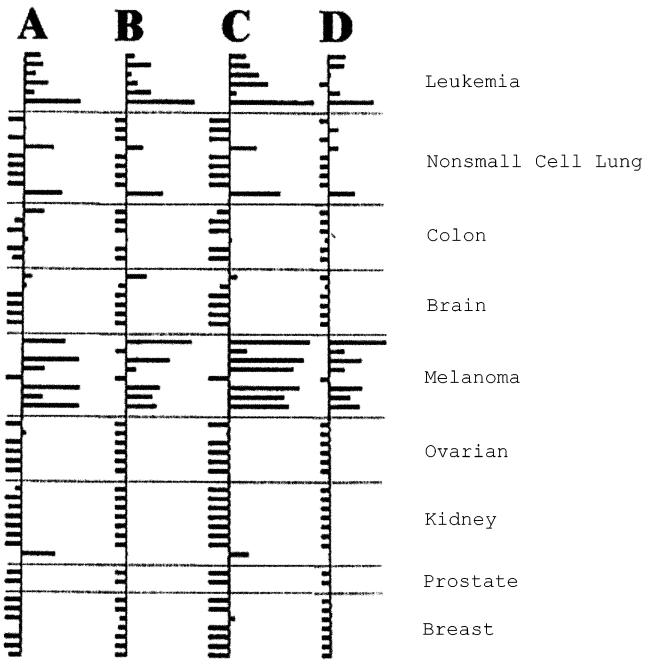

Figure 5. Total growth inhibition (TGI)-based mean-graph profiles derived from testing of bafilomycin A_1 (A), salicylihalamide A (B), lobatamide A (C), and oximidine II (D) in the NCI 60-cell screen. Each horizontal bar represents the sensitivity of an individual cell line relative to the average sensitivity (represented by the central vertical line) of the full 60-cell panel. Bars projecting to the right represent relatively more sensitive cell lines, and bars to the left less sensitive lines. Reprinted with permission from ref 48. Copyright 2001 American Soceity for Pharmacology and Experimental Therapeutics.

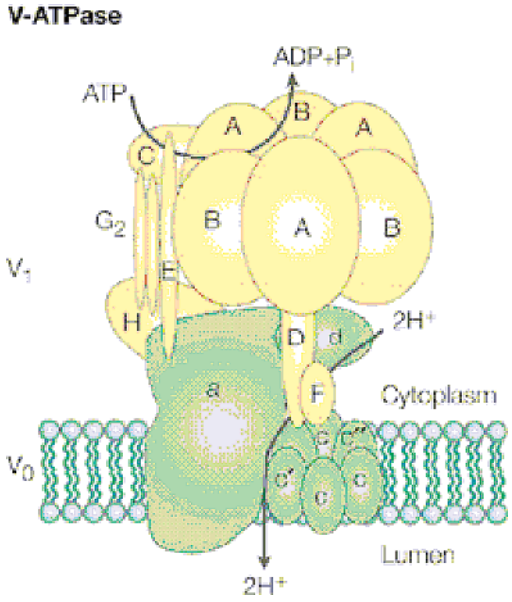

Figure 6. Structure of V-ATPases. ATP hydrolysis by th eperipheral V_1 domain (shown in yellow) drives proton transport through the integral V_0 domain (shown in green) from the cytoplasm to the lumen. Reprinted with permission from ref 49d. Copyright 2002 Nature Publishing Group (http://www.nature.com/).

Smith and Zheng have screened salicylihalamide analogues such as **207** and **208** for in vitro activity against a series of cell lines for their growth inhibitory activity.[23a] Analogues **207** and **208** both retained significant, albeit attenuated activity. They observed that removal of the double bond reduces the activity slightly on several cell lines, and they suggested that the structure elements on the lactone ring might be important, but not critical for activity. They hypothesized that their function is to orchestrate the optimal orientation between the side chain and salicylate substituents for receptor binding.

Table 3. Inhibition of the Proton (H^+) Transport Activity of Reconstituted V-ATPase from Bovine Brain by Synthetic Salicylihalamides and Its Congeners

compd	IC_{50} (nM)	compd	IC_{50} (nM)
1a	270	**199**	1.6
2a	<1.0	**200**	1.8
192	230	**201**	>1000
193	3.7	**202**	1000
194	1.2	**203**	3.0
195	3.0	**204**	30
196	1.0	**205**	300
197	<1.0	**206**	180
198	1.0		

Table 4. Growth Inhibition of the SK-MEL 5 Human Melanoma Cell Line by Synthetic Salicylihalamides and Its Congeners

compd	IC_{50} (μM)	compd	IC_{50} (μM)
2a	0.06	**199**	0.5
192	>20	**200**	0.45
193	0.04	**201**	1.5
194	0.1	**202**	>20
195	0.6	**203**	8
196	0.38	**204**	>20
197	0.3	**205**	1
198	0.3	**206**	>20

7. Biology of Apicularen A and Synthetic Analogues

Kunze and co-workers have shown that apicularen A (**3**) had very high cytostatic activity, with IC_{50} values ranging between 0.3 and 3.0 nM with nine different human cancer cell lines, including the multidrug-resistant line KB-V1 (Table 6).[7] They further showed the dose−response study of apicularen A (**3**) with the continuously growing KB-3-1 cell line, established from a primary cervix carcinoma, with an IC_{50} value of 1.0 nM. When the culture medium was replaced by fresh medium without **3**, the KB-3-1 cells started to propagate again without delay.

De Brabander and co-workers demonstrated the utility of synthetic apicularen A (**3**) and analogous compounds against the growth inhibitory properties of the melanoma cell line SK-MEL-5.[35] As shown in Table 7, apicularen A (**3**) is about 5-fold more potent at 6 nM than (−)-salicylihalamide A (**2a**) at 30 nM. Some variations, including C-11 epimers (**112**), a geometrical isomer (**110**), and *N*-pivaloyl (**111**), *N*-hexanoyl (**209**), and *N*-carbamoyl (**210**) enamine derivatives (Figure 8), can be accommodated with only a modest loss of activity. The inability of compounds **211** and **212** to arrest cell growth indicates that there may be a specific role for the *N*-acyl enamine moiety in the growth inhibition.

8. Biology of Simplified Lobatamide Analogues

Boyd and co-workers have shown that lobatamide A had a COMPARE pattern algorithm similar to that

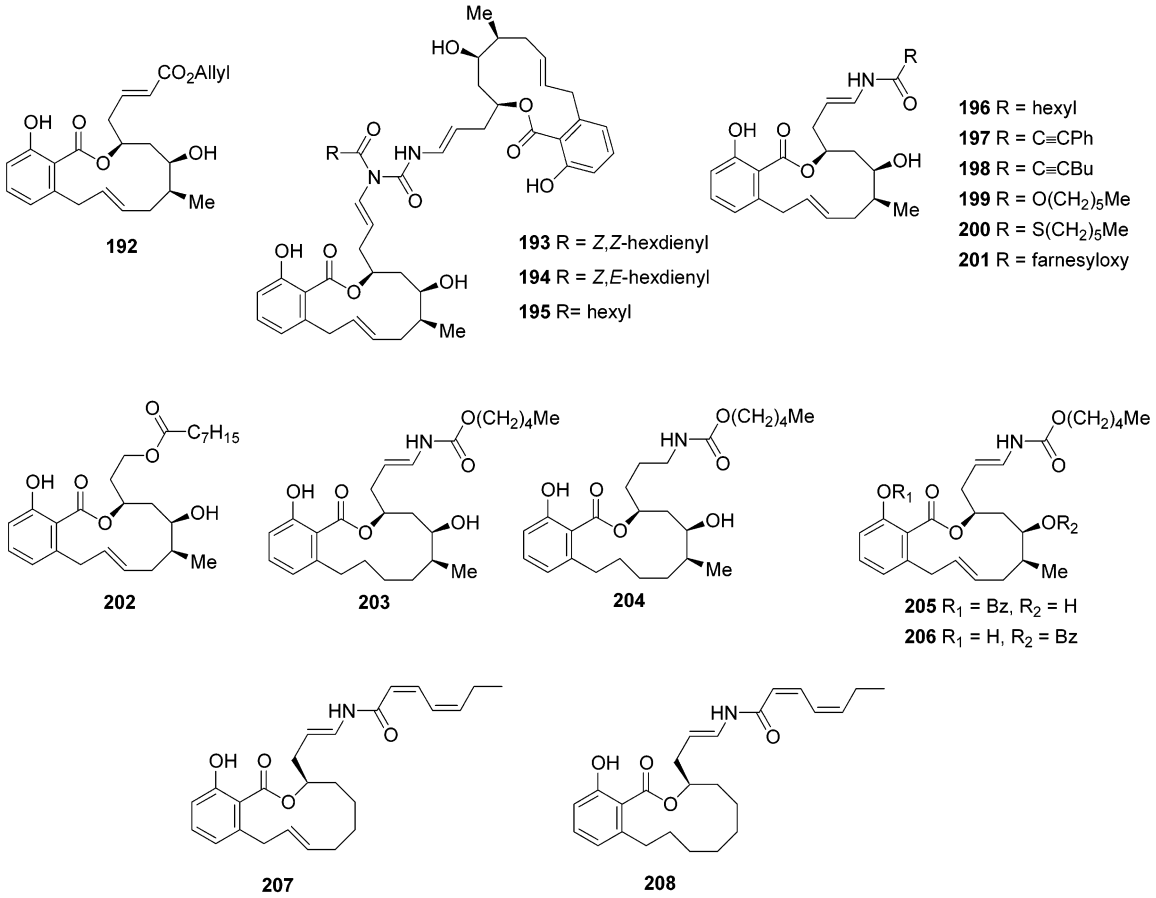

Figure 7. Structures of salicylihalamide A derivatives.

Table 5. Biological Evaluation of Salicylihalamide A and Analogues 207 and 208

		GI_{50} ($\times 10^{-2}$ μM)		
cell type	cell line	**2a**	**207**	**208**
panacreas-a	BXPC-3	8.0	46	88
breast adn	MCF-7	7.4	57	48
CNS gliobl	SF268	8.0	11	37
lung-NSC	NCI-H460	7.3	56	65
colon	KM20L2	3.8	15	71
prostate	DU-145	8.1	87	78

Table 6. Cytostatic Effects of Apicularen A on Human Cell Lines

cell line	cell origin	IC_{50} (nM)
KB-3-1	cervix carcinoma	1.0
KB-V1	cervix carcinoma	0.4
K-562	chronic myelogenous leukemia	2.0
HL-60	acute myeloid leukemia	3.0
U-937	histocytic carcinoma	1.5
A-498	kidney carcinoma	0.3
A-549	lung carcinoma	0.1
PC-3	prostate carcinoma	0.5
SK−OV-3	ovarian carcinoma	1.5

of salicyliahamide A (**2a**) and oximidine II (**6b**, see Table 2 and Figure 5).[48] This suggested that the lobatamides may act by a novel mechanism of action since their activity profiles did not correlate using COMPARE with compounds in the NCI database whose mechanism of action are known.

Porco and co-workers synthesized and studied V-ATPase inhibition with a series of simplified lobatamide analogues.[52] Since previous studies have

Table 7. Growth Inhibition of the SK-MEL 5 Human Melanoma Cell Line by Apicularen A and Analogues

compd	IC_{50} (μM)	compd	IC_{50} (μM)
2a	0.03	**209**	7.5
3	0.006	**210**	0.5
110	0.06	**211**	>20
111	0.9	**212**	>20
112	0.45		

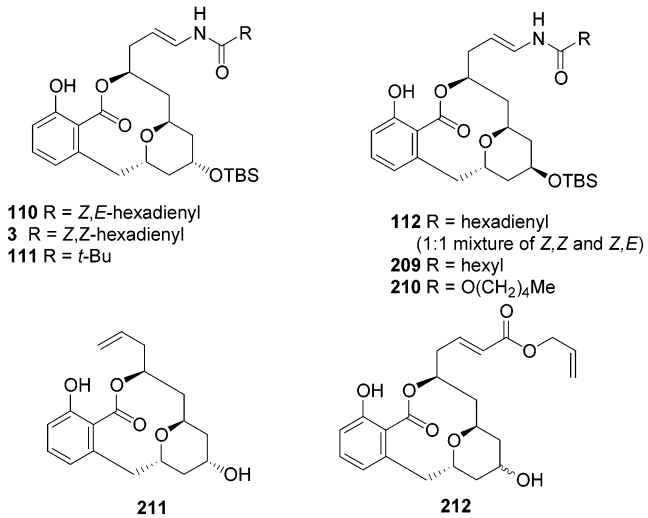

Figure 8. Structures of apicularen A derivatives.

shown that the enamide side chain is important for the potent bioactivities of salicylihalamides[19a,51] and apicularen A,[35] the Porco group initiated studies exploring variations of the C1−C8 subunit of the

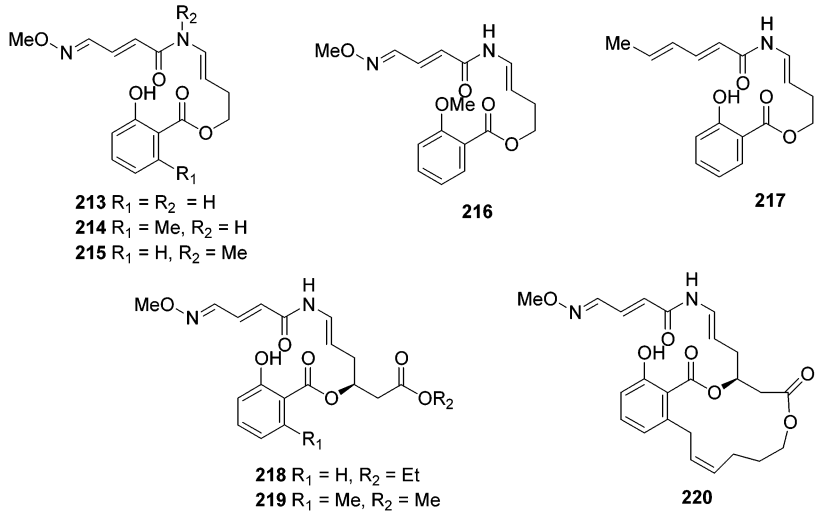

Figure 9. Structures of lobatamide A derivatives.

Table 8. Effect of Simplified Analogues of Lobatamides against Bovine V-ATPase

compd	IC_{50} (μM)	compd	IC_{50} (μM)
4b	0.002	**217**	*b*
213	*a*	**218**	18
214	1.3	**219**	0.1
215	200	**220**	1.2
216	no effect		

[a] 25% inhibition at 20 μM; higher concentrations not soluble. [b] 25% inhibition at 30 μM; higher concentrations not soluble.

Table 9. IC_{50} Values of Macrocyclic Lactones against Normal and Transformed Rat 3Y1 Fibroblasts

		IC_{50} (nM)			
cell line	oncogene	**2a**	**4a**	**6a**	**6b**
3Y1		770	150	510	270
SV-3Y1	SV40 large T	73	31	740	350
E1A-3Y1	E1A	30	11	30	17
Ad12-3Y1	E1A, E1B	32	13	62	36
HR-3Y1	v-H-*ras*	190	43	16	9.0
SR-3Y1	v-*src*	41	12	27	14

lobatamides. The first simplified lobatamide analogues (Figure 9) were evaluated for activity against bovine V-ATPase activity. Minimally functionalized salicylate enamide compounds **213** and **217** were found to only weakly inhibit bovine V-ATPase (25% inhibition at 20 μM and 30 μM, respectively), as shown in Table 8. Simple permutation of the ortho hydrogen to a methyl group regained much of the activity (**214**, IC_{50} = 1.3 μM), whereas methylated analogues **215** and **216** showed no inhibition of V-ATPase at all, indicating the importance of both a free phenol OH and enamide NH functionalities. Macrolactone **220** showed good V-ATPase inhibition (1.2 μM), but not the nanomolar potency of the lobatamide C (**4b**), which indicates that the ring size and substitution of the macrolactone are important for potent V-ATPase inhibition. The only reasonably potent simplified salicylate enamide analogue was carboxymethyl compound **219** (0.1 μM), 180 times more active than unsubstituted carboxyethyl compound **218** but 50 times less active than lobatamide C (**4b**). Even though these simplified derivatives were much less potent versus the natural products, a number of useful SARs have been uncovered, including enhancement of V-ATPase inhibition in acyclic analogues by ortho substitution of the salicylate ring.

9. Biology of Oximidines I and II

Hayakawa and co-workers have studied the antitumor effects of oximidines I (**6a**) and II (**6b**) using normal and transformed 3Y1 rat fibroblasts.[10] Oximidines I (**6a**) and II (**6b**) inhibited the growth of 3Y1 cells transformed with the adenovirus E1A, v-H-*ras*, and v-*src* oncogenes at concentrations 15- to 30-fold lower than that of the parent 3Y1 cells (Table 9). The SV40 oncogene cell line showed almost the same sensitivity as the normal cells. By flow cytometric analysis, the authors were able to reveal that **6a** arrested the cell cycle of *ras*- and *src*-transformed 3Y1 cells at the G1 phase. Boyd and co-workers also showed similar results with salicylihalamide A (**2a**) and lobatamide A (**4a**) within this study.[48] However, these two compounds had good inhibitory activity with the SV40 oncogene cell line.

10. Conclusions and Future Prospects

This review has discussed a new class of salicylate macrolactone enamide natural products with a new mode of biological activity. Total syntheses of salicylihalamide A and its congeners have led to the identification of further classes of compounds aimed at developing mammalian V-ATPase as a therapeutic target. Since the initial discovery of these compounds just 6 years ago, academic laboratories around the world have taken a keen interest in the unique chemistry and biology of these novel new chemical entities. These targets will serve as attractive chemical entities for drug discovery research in the pharmaceutical sector, especially in the area of oncology. Many of these compounds have achieved nanomolar potency against its putative target, and there is great potential that future pharmaceutical drug discovery programs will occur in this area. What will expand this area of research even more will largely depend on the shorter syntheses of these types of compounds, so that more extensive structure−activity relation-

ships can be explored. Newly isolated natural products will continue to fuel future synthetic studies as well as provide opportunities for molecular probes at human protein targets of disease states.

11. Acknowledgments

The author thanks Drs. R. Jason Herr and Peter R. Guzzo of Albany Molecular Research, Inc. for critical reading of this manuscript and for their many valuable suggestions.

12. Abbreviations/Definitions

Ac	acetyl
AIBN	2,2′-azobisisobutyronitrile
9-BBN	9-borabicyclo[3.3.1]nonane
BINAP	[1,1′-binaphalene]-2,2′-diylbis(diphenylphosphane)
Bn	benzyl
Bu	butyl
CSA	chlorosulfonic acid
CuTC	copper(I) thiophene carboxylate
dba	dibenzylideneacetone
DBU	1,8-diazabicyclo[5.4.0]undec-7-ene
DCC	dicyclohexylcarbodiimide
DDQ	2,3-dichloro-5,6-dicyano-1,4-benzoquinone
DEAD	diethylazodicarboxylate
DEIPS	diethylisopropylsilyl
DIAD	diisopropylazodicarboxylate
DIBALH	diisobutylaluminum hydride
DMA	*N*,*N*-dimethylacetamide
DMAP	4-(dimethylamino)pyridine
DMF	*N*,*N*-dimethylformamide
DMPU	1,3-dimethyl-3,4,5,6-tetrahydro-2(1*H*)-pyrimidone
DMSO	dimethyl sulfoxide
dppf	1,1′-bis(diphenylphosphanyl)ferrocene
EDTA	ethylenediaminetetraacetic acid
GI_{50}	concentration that inhibits growth of cells by 50%
HMDS	hexamethyldisilazanide
HMPA	hexamethylphosphoramide
IC_{50}	concentration that kills 50% of cells
Im	imidazolyl
i-Pr	isopropyl
Ipc	isopinocampheyl
LDA	lithium diisopropylamide
LICA	lithium(cyclohexyl)(isopropyl)amide
Ms	methanesulfonyl
MOM	methoxymethyl
NBS	*N*-bromosuccinimide
NCI	National Cancer Institute
NMO	4-methylmorpholine oxide
NMP	*N*-methylpyrrolidone
NPS	*N*-phenylselenyl
PMB	*p*-methoxylbenzyl
PPTS	pyridinium *p*-toluenesulfonate
TBAF	tetra-*n*-butylammonium fluoride
TBS	*tert*-butyldimethylsilyl
TBSOTf	*tert*-butyldimethylsilyl trifluoromethanesulfonate
Tc	thiophene-2-carboxylate
TES	triethylsilyl
Tf	trifluoromethanesulfonyl
TFA	trifluoroacetic acid
Tf_2O	trifluoromethanesulfonic anhydride
TFP	tri(furyl)phosphine
TGI	concentration that totally inhibits growth of cells
THF	tetrahydrofuran
TIPS	triisopropylsilyl
TMS	trimethylsilyl
TPAP	tetrapropylammonium perruthenate
TPS	triphenylsilyl
Ts	*p*-toluenesulfonyl
p-TsOH	*p*-toluenesulfonic acid

13. References

(1) For reviews on the influence of natural products isolation upon drug discovery, see: (a) Newmann, D. J.; Cragg, G. M.; Snader, K. M. *Nat. Prod. Rep.* **2000**, *17*, 215. (b) Kingston, D. G.; Newman, D. J. *Curr. Opin. Drug Discuss. Dev.* **2002**, *5*, 304. (c) Breinbauer, R.; Vetter, I. R.; Waldmann, H. *Angew. Chem., Int. Ed.* **2002**, *41*, 2879.

(2) For recent reviews on solution- and solid-phase strategies toward the synthesis of libraries based on natural product templates, and syntheses of natural product-like libraries, see: (a) Hall, D. G.; Manku, S.; Wang, F. *J. Comb. Chem.* **2001**, *3*, 125. (b) Arya, P.; Joseph, R.; Chou, D. T. H. *Chem. Biol.* **2002**, *9*, 145. (c) Arya, P.; Baek, M.-G. *Curr. Opin. Chem. Biol.* **2001**, *5*, 292. (d) Breinbauer, R.; Manger, M.; Scheck, M.; Waldmann, H. *Curr. Med. Chem.* **2002**, *9*, 2129.

(3) For comprehensive surveys of combinatorial library synthesis, see: (a) Dolle, R. E. *Mol. Diversity* **1998**, *3*, 199. (b) Dolle, R. E. *J. Comb. Chem.* **1999**, *1*, 235. (c) Dolle, R. E. *J. Comb. Chem.* **2000**, *2*, 383. (d) Dolle, R. E. *J. Comb. Chem.* **2001**, *3*, 477. (e) Dolle, R. E. *J. Comb. Chem.* **2002**, *4*, 369. (f) Bhattacharyya, S. *Curr. Med. Chem.* **2001**, *8*, 1383.

(4) Grifo, F.; Newman, D.; Fairfield, A. S.; Bhattaharya, B.; Grupenhoff, J. T. The Origins of Prescription Drugs. In *Biodiversity and Human Health*; Grifo, F., Rosenthal, J., Eds.; Island Press: Washington, DC, 1997; p 131.

(5) Erickson, K. L.; Beutler, J. A.; Cardellina, J. H., II; Boyd, M. R. *J. Org. Chem.* **1997**, *62*, 8188.

(6) Erickson, K. L.; Beutler, J. A.; Cardellina, J. H., II; Boyd, M. R. *J. Org. Chem.* **2001**, *66*, 1532.

(7) (a) Kunze, B.; Jansen, R.; Sasse, F.; Höfle, G.; Reichenbach, H. *J. Antibiot.* **1998**, *51*, 1075. (b) Jansen, R.; Kunze, B.; Reichenbach, H.; Höfle, G. *Eur. J. Org. Chem.* **2000**, 913.

(8) McKee, T. C.; Galinis, D. L.; Pannell, L. K.; Cardellina, J. H., II.; Laakso, J.; Ireland, C. M.; Murray, L.; Capon, R. J.; Boyd, M. R. *J. Org. Chem.* **1998**, *63*, 7805.

(9) Dekker, K. A.; Aiello, R. J.; Hirai, H.; Inagaki, T.; Sakakibara, T.; Suzuki, Y.; Thompson, J. F.; Yamauchi, Y.; Kojima, N. *J. Antibiot.* **1998**, *51*, 14.

(10) Kim, J. W.; Shin-ya, K.; Furihata, K.; Hayakawa, Y.; Seto, H. *J. Org. Chem.* **1999**, *64*, 153.

(11) Isolation and structure of zearalenone: (a) Stob, M.; Baldwin, R. S.; Tuite, J.; Andrews, F. N.; Gillette, K. G. *Nature* **1962**, *196*, 1318. (b) Urry, W. H.; Wehrmeister, H. L.; Hodge, E. B.; Hidy, P. H. *Tetrahedron Lett.* **1966**, 3109. (c) Cordier, C.; Gruselle, M.; Jaouen, G.; Hughes, D. W.; McGlinchey, M. J. *Magn. Reson. Chem.* **1990**, *28*, 835.

(12) Previous syntheses of zearalenone: Fürstner, A.; Thiel, O. R.; Kindler, N.; Bartkowska, B. *J. Org. Chem.* **2000**, *65*, 7990 and references therein.

(13) Isolation and structure of radicicol and monocillin: (a) Delmotte, P.; Delmotte-Plaquée, J. *Nature* **1953**, *171*, 344. (b) Ayer, W. A.; Lee, S. P.; Tsuneda, A.; Hiratsuka, Y. *Can. J. Microbiol.* **1980**, *26*, 766. (c) Cutler, H. G.; Arrendale, R. F.; Springer, J. P.; Cole, P. D.; Roberts, R. G.; Hanlin, R. T. *Agric. Biol. Chem.* **1987**, *51*, 3331.

(14) Previous syntheses of radicicol and monocillin: (a) Lampilas, M.; Lett, R. *Tetrahedron Lett.* **1992**, *33*, 773, 777. (b) Garbaccio, R. M.; Stachel, S. J.; Baeschilin, D. K.; Danishefsky, S. J. *J. Am. Chem. Soc.* **2001**, *123*, 10903.

(15) Roe, S. M.; Prodromou, C.; O'Brien, R.; Ladbury, J. E.; Piper, P. W.; Pearl, L. H. *J. Med. Chem.* **1999**, *42*, 260.

(16) For reviews on the ring-closing metathesis reaction, see: (a) Grubbs, R. H.; Pine, S. H. In *Comprehensive Organic Synthesis*; Trost, B. M., Ed.; Pergamon: New York, 1991; Vol. 5, Chapter 9. (b) Schmalz, H.-G. *Angew. Chem., Int. Ed.* **1995**, *34*, 1833. (c) Schuster, M.; Blechert, S. *Angew. Chem., Int. Ed.* **1997**, *36*, 2036. (d) Grubbs, R. H.; Chang, S. *Tetrahedron* **1998**, *54*, 4413. (e) Armstrong, S. A. *J. Chem. Soc., Perkin Trans. 1* **1998,** 371. (f) Randall, M. L.; Snapper, M. L. *J. Mol. Catal. A: Chem.* **1998**, *133*, 29. (g) Pariya, C.; Jayaprakash, K. N.; Sarkar, A. *Coord. Chem. Rev.* **1998**, *168*, 1. (h) Phillips, A. J.; Abell, A. D. *Aldrichim. Acta* **1999**, *32*, 75. (i) Wright, D. L. *Curr. Org. Chem.* **1999**, *3*, 211. (j) Fürstner, A. *Angew. Chem., Int. Ed.* **2000**, *39*, 3013. (k) Trnka, T. M.; Grubbs, R. H. *Acc. Chem. Res.* **2001**, *34*, 18.

(17) (a) Fürstner, A.; Thiel, O. R.; Blanda, G. *Org. Lett.* **2000**, *2*, 3731. (b) Fürstner, A.; Dierkes, T.; Thiel, O. R.; Blanda, G. *Chem. Eur. J.* **2001**, 5286.
(18) Snider, B. B.; Song, F. *Org. Lett.* **2001**, *3*, 1817.
(19) (a) Wu, Y.; Liao, X.; Wang, R.; Xie, X.-S.; De Brabander, J. K. *J. Am. Chem. Soc.* **2002**, *124*, 3245. (b) Wu, Y.; Esser, L.; De Brabander, J. K. *Angew. Chem., Int. Ed.* **2000**, *39*, 4308. (c) Bhattacharjee, A.; De Brabander, J. K. *Tetrahedron Lett.* **2000**, *41*, 8069.
(20) Labrecque, D.; Charron, S.; Rej, R.; Blais, C.; Lamothe, S. *Tetrahedron Lett.* **2001**, *42*, 2645.
(21) Georg, G. I.; Ahn, Y. M.; Blackman, B.; Farokhi, F.; Flaherty, P. T.; Mossman, C. J.; Roy, S.; Yang, K. *J. Chem. Soc., Chem. Commun.* **2001**, 255.
(22) (a) De Silva, S. O.; Reed, J. N.; Billedeau, R. J.; Wang, X.; Norris, D. J.; Snieckus, V. *Tetrahedron* **1992**, *48*, 4863. (b) Bibi, M. P.; Miah, M. A. J.; Snieckus, V. *J. Org. Chem.* **1984**, *49*, 737.
(23) (a) Smith, A. B., III; Zheng, J. *Tetrahedron* **2002**, *58*, 6455. (b) Smith, A. B., III; Zheng, J. *Synlett* **2001**, 1019.
(24) Masamune, S.; Ma, P.; Okumoto, H.; Ellingobe, J. W.; Ito, Y. *J. Org. Chem.* **1984**, *49*, 2837.
(25) Kermadec, K.; Prudhomme, M. *Tetrahedron Lett.* **1993**, *34*, 2757.
(26) Myers, A. G.; Yang, B. H.; Chen, H.; McKinstry, L.; Kopecky, D. J.; Gleason, J. L. *J. Am. Chem. Soc.* **1997**, *119*, 6496.
(27) (a) Lee, A. W. M.; Chan, W. H.; Wong, H. C.; Wong, M. S. *Synth. Commun.* **1989**, *19*, 547. (b) Patroni, J. J.; Stick, R. V. *Aust. J. Chem.* **1978**, *31*, 445. (c) Iacono, I.; Rasmussen, J. R.; Card, J.; Smart, B. E. *Organic Syntheses*; Wiley & Sons: New York, 1993; Collect. Vol. VII, p 139.
(28) For a selected example of reversible olefin metathesis reactions, see: Fürstner, A.; Thiel, O. R.; Ackermann, L. *Org. Lett.* **2001**, *3*, 449 and references therein.
(29) (a) Sanford, M. S.; Love, J. A.; Grubbs, R. H. *J. Am. Chem. Soc.* **2001**, *123*, 6543. (b) Ulman, M.; Grubbs, R. H. *J. Org. Chem.* **1999**, *64*, 7202.
(30) Bauer, M.; Maier, M. E. *Org. Lett.* **2002**, *4*, 2205.
(31) Duthaler, R. O.; Herold, P.; Lottenbach, W.; Oertle, K.; Riediker, M. *Angew. Chem., Int. Ed.* **1989**, *28*, 495.
(32) Formal total synthesis: Holloway, G. A.; Hügel, H. M.; Rizzacasa, M. A. *J. Org. Chem.* **2003**, *68*, 2200. Model studies: Feutrill, T.; Holloway, G. A.; Hilli, F.; Hügel, H. M.; Rizzacasa, M. A. *Tetrahedron Lett.* **2000**, *41*, 8569.
(33) Drouet, K. E.; Theodorakis, E. A. *Chem. Eur. J.* **2000**, *6*, 1987.
(34) Bhattacharjee, A.; De Brabander, J. K. *Tetrahedron Lett.* **2000**, *41*, 8069.
(35) Bhattacharjee, A.; Seguil, O. R.; De Brabander, J. K. *Tetrahedron Lett.* **2001**, *42*, 1217.
(36) (a) Lewis, A.; Stefanuti, I.; Swain, S. A.; Smith, S. A.; Taylor, R. J. K. *Tetrahedron Lett.* **2001**, *42*, 5549. (b) Lewis, A.; Stefanuti, I.; Swain, S. A.; Smith, S. A.; Taylor, R. J. K. *Org. Biomol. Chem.* **2003**, *1*, 104.
(37) Nicolaou, K. C.; Kim, D. W.; Baati, R. *Angew. Chem., Int. Ed.* **2002**, *41*, 3701.
(38) Hilli, F.; White, J. M.; Rizzacasa, M. A. *Tetrahedron Lett.* **2002**, *43*, 8507.
(39) White, J. D.; Blakemore, P. R.; Browder, C. C.; Hong, J.; Lincoln, C. M.; Nagorny, P. A.; Robarge, L. A.; Wardrop, D. J. *J. Am. Chem. Soc.* **2001**, *123*, 8593.
(40) Kuhnert, S. M.; Maier, M. E. *Org. Lett.* **2002**, *4*, 643.
(41) Brunner, H.; Lautenschlager, H.-H. *Synthesis* **1989**, 706.
(42) (a) Shen, R.; Lin, C. T.; Porco, J. A., Jr. *J. Am. Chem. Soc.* **2002**, *124*, 5650. (b) Shen, R.; Lin, C. T.; Bowman, E. J.; Bowman, B. J.; Porco, J. A., Jr. *J. Am. Chem. Soc.* **2003**, *125*, 7889.
(43) For synthetic studies to enamide side chains, see: (a) Snider, B. B.; Song, F. *Org. Lett.* **2000**, *2*, 407. (b) Kuramochi, K.; Watanabe, H.; Kitahara, T. *Synlett* **2000**, 397. (c) Shen, R.; Porco, J. A., Jr. *Org. Lett.* **2000**, *2*, 1333. (d) Stefanuti, I.; Smith, S. A.; Taylor, R. J. K. *Tetrahedron Lett.* **2000**, *41*, 3735. (e) Fürstner, A.; Brehm, C.; Cancho-Grande, Y. *Org. Lett.* **2001**, *3*, 3955.
(44) Coleman, R. S.; Garg, R. *Org. Lett.* **2001**, *3*, 3487.
(45) Scheufler, F.; Maier, M. E. *Synlett* **2001**, 1221.
(46) Wang, X.; Porco, J. A., Jr. *J. Am. Chem. Soc.* **2003**, *125*, 6040.
(47) (a) Boyd, M. R. In *Cancer: Principles and Practice of Oncology Updates;* DeVita, V. T., Hellman, S., Jr., Rosenberg, S. A., Eds.; Lippincott: Philadelphia, 1989; Vol. 3, No. 10, pp 1−12. (b) Boyd, M. R. In *Anticancer Drug Development Guide: Preclinical Screening, Clinical Trials and Approvals*; Teicher, B., Ed.; Humana Press: Towata, NY, 1997; pp 23−42. (c) Boyd, M. R.; Paull, K. *Drug. Dev. Res.* **1995**, *34*, 91. (d) Weinstein, J. N.; Myers, T. G.; O'Connor, P. M.; Friend, S. H.; Fornace, A. J., Jr.; Kohn, K.; Fojo, T.; Bates, S. E.; Rubinstein, L. V.; Anderson, N. L.; Buolamwini, J. K.; van Osdol, W.; Monks, A. P.; Scudiero, D. A.; Sausville, E. A.; Zaharevitz, D. W.; Bunow, B.; Viswanadan, V. N.; Johnson, G. W.; Wittes, R. E.; Paull, K. D. *Science* **1997**, *275*, 343.
(48) Boyd, M. R.; Farina, C.; Belfiore, P.; Gagliardi, S.; Kim, J. W.; Hayakawa, Y.; Beutler, J. A.; McKee, T. C.; Bowman, B. J.; Bowman, E. J. *J. Pharmacol. Exp. Ther.* **2001**, *297*, 114.
(49) For reviews on V-ATPases, see: (a) Forgac, M. *Adv. Mol. Cell. Biol.* **1998**, *23B*, 403. (b) Farina, C.; Gagliardi, S. *Drug Discovery Today* **1999**, *4*, 163. (c) Keeling, D. J.; Herslof, M.; Ryberg, B.; Sjogren, S.; Solvell, L. *Ann. N.Y. Acad. Sci.* **1997**, *834*, 600. (d) Nishi, T.; Forgac, M. *Nat. Rev. Mol. Cell Biol.* **2002**, *3*, 94. (e) Beutler, J. A.; McKee, T. C. *Curr. Med. Chem.* **2003**, *10*, 789.
(50) (a) Bowman, E. J.; Seibers, A.; Altendorf, K. *Proc. Natl. Acad. Sci. U.S.A.* **1988**, *85*, 7972. (b) Dröse, S.; Altendorf, K. *J. Exp. Biol.* **1997**, *200*, 1.
(51) Wu, Y.; Seguil, O. R.; De Brabander, J. K. *Org. Lett.* **2000**, *2*, 4241.
(52) Shen, R.; Lin, C. T.; Bowman, E. J.; Bowman, B. J.; Porco, J. A., Jr. *Org. Lett.* **2002**, *4*, 3103.

CR030035S